Research Article

For reprint orders, please contact: reprints@future-science.com

Future Medicinal Chemistry

Synthesis, anticancer activity, structure–activity relationship and binding mode of interaction studies of substituted pentanoic acids

Sanchita Dutta[1,2], Amit Kumar Halder[1], Nilanjan Adhikari[1], Sk. Abdul Amin[1], Sanjib Das[1], Achintya Saha[2] & Tarun Jha*[,1]

[1]Natural Science Laboratory, Division of Medicinal & Pharmaceutical Chemistry, Department of Pharmaceutical Technology, Jadavpur University, PO Box 17020, Kolkata 700032, West Bengal, India

[2]Department of Chemical Technology, University of Calcutta, 92 APC Ray Road, Kolkata 700009, India

*Author for correspondence: tjupharm@yahoo.com

Aim: Simultaneous inhibition of MMP-2 and HDAC8 may be an effective strategy to target cancer. **Methodology:** In continuation of our earlier efforts, a series of substituted pentanoic acids (**1–18**) were synthesized and checked for their biological activity along with some earlier reported compounds (**19–35**). **Results:** Compounds **18** and **31** were found to induce apoptosis effectively in a dose-dependent fashion in Jurkat-E6.1 cell line. They reduced the expression of both MMP-2 and HDAC8 effectively. **31** also produced prominent intensity of fluorescence to bring nick in Jurkat-E6.1 cells. **31** also showed cellular arrest in sub-G0 phase. **Conclusion:** Such compounds may be useful to battle against cancer.

First draft submitted: 30 July 2018; Accepted for publication: 26 April 2019; Published online: 2 August 2019

Keywords: apoptosis • cell cycle • cytotoxicity • flow cytometry • leukemia • metalloenzyme • mitochondrial membrane potential • molecular docking • pentanoic acid • SAR

Zinc-dependent metalloenzymes such as MMPs, HDACs and APN have been implicated in cancer cell progression, differentiation, migration, invasion, metastatis and angiogenesis [1–18]. Ranogajec et al. [6] exhibited that the combined expression of APN, MMP-2 and MMP-9 along with other related factors may serve as the poor prognosis for breast cancer patients. Moreover, APN has also been found to exert a positive correlation with the MMP-2 expression as well as cellular migration as evidenced in ovarian cancer (OVCA) cell lines [19]. Again, small interfering ribonucleic acid (siRNA)-mediated silencing of APN markedly decrease the VEGF expression along with a down regulation of MMP-2 as seen in OVCA cells [19]. Liu *et al.* explored that 14-3-3σ protein-induced expression of MMPs are related to APN in hepatocellular cancer [20]. Nevertheless, silencing of APN produces an abrogating r14-3-3σ-protein that stimulated the expression of MMPs including MMP-2 and -9 in HS68 fibroblasts [20]. Western blot analysis revealed that APN signalling has been involved in the activation of nuclear factor (NF)-κB and NF-κB further regulates MMP-2 and MMP-9 through mediating PI3K and MAPK pathways as seen in the osteosarcoma cell line [21]. Therefore, treatment with APN inhibitor bestatin decreases all these APN, MMP-2 and MMP-9 enzymatic activities along with their mRNA expression [21]. Recently, Amin *et al.* [7] proposed the utility of simultaneous dual inhibition of MMP-2 and HDAC8 for combating haematological malignancies. Nevertheless, HDAC inhibitors has also been found to decrease the activity of MMP-2 activation along with cellular invasion of lung cancer through upregulation of the reversion-inducing-cysteine-rich protein with kazal motifs (RECK) [3,22]. RECK has been established to exert inhibitory mechanisms on the activity of MMP-2 and MMP-9 enzymes [22–25], crucial regulators of tumor growth, cell proliferation, angiogenesis and apoptosis [26]. Oh *et al.* [25] also suggested that RECK is directly involved in the reduction of active MMP-2 in HT1080 fibrosarcoma cell line. RECK is also found to suppress the release of pro-MMP-9 and subsequently hinders metastasis and invasion of tumor cells [24]. Nevertheless, an inverse correlation between RECK expression and activation of MMP-2 has also been established [23]. Not only that, tumors having higher RECK expression reveal a lower expression of

newlands press

MMP-9 [23,27–29]. Again, lower expression of RECK is highly correlated with the higher expression of MMP-2 and MMP-9 in a variety of cancers including prostate, breast, lungs and stomach cancer, as well as squamous carcinoma and osteosarcoma [30,31]. Higher expression of RECK has a positive impact on the survival of cancer patients while lower expression is correlated with the poor prognosis of cancer patients [30,31]. Again, Jeon and Lee explored that under hypoxic condition, RECK expression has been restored by HDAC inhibition which further inhibits the cancer cell invasion and migration through downregulation of MMP-2 and MMP-9 [32]. Trichostatin (TSA), a class I HDAC inhibitor, found to reduce the level of gelatinase (both MMP-2 and -9) in esophageal squamous cell carcinoma [33,34]. Moreover, class I HDAC inhibitor PD-106 was found to reduce the MMP-2 expression [33]. Mani *et al.* [33] demonstrated that class I HDACs have a significant importance in the expression of MMP-2 through modulating MMP-2/tissue inhibitor of MMP-2 (TIMP-2) complex or mediating the expression of TIMP-2 and membrane type 1-MMP (MT1-MMP; also known as MMP-14). Therefore, it may be postulated that compounds inhibiting these metalloenzymes may be a valuable weapon for the crusade against cancer. Earlier our research group has explored a number of pentanoic acid derivatives as dual inhibitors of MMP-2 and HDAC8 having potential antimigratory and antiinvasive properties in non-small-cell lung cancer (NSCLC) A549 cell line [3]. It has also been proposed that compounds inhibiting multiple metalloenzymes (namely MMP-2, MMP-9, HDAC8) may be more effective to battle against cancer [3]. However, it has been suggested that the potential HDAC8 inhibitors may be effective against cancer [35] and HDAC8 inhibitors down regulate the expression of both MMP-2 and MMP-9 via RECK expression [22–25]. Therefore, in this current study, a number of pentanoic acid derivatives were synthesized, biologically evaluated and structure–activity relationship (SAR) was done and subsequently, subjected to molecular docking interactions to justify and validate these propositions to get useful anticancer agents.

Materials & methods

Chemicals & reagents

The analytical grade chemicals as well as media and antibodies were used to perform this study. Different media for cell culture study such as RPMI-1640 and Dulbecco's modified Eagle medium (DMEM) as well as fetal bovine serum (FBS) and different antibiotics (namely penicillin and streptomycin) were purchased from Gibco, BRL (NY, USA). All tissue culture plastic wares used in this study were purchased from BD Bioscience (CA, USA). Different molecular biology grade solvents were used for this purpose. Moreover, chemicals such as MTT, PI, RNAase and 4′,6-diamidino-2 phenylindole (DAPI) were purchased from Sigma-Aldrich (MO, USA). JC1 assay kit was obtained from BD Bioscience. Annexin V-FITC kit was purchased from Calbiochem (Darmstadt, Germany). Anti MMP-2, Anti HDAC8 monoclonal antiboby and anti rabit FITC conjugated secondary antibody used were from Santa Cruz Biotechnology Inc. (CA, USA).

Synthesis

All these compounds were synthesized following the broad protocol proposed by Halder and co-workers [3]. The general method of synthesis of these pentanoic acid derivatives was outlined in Figure 1 .

Synthetic procedure of substituted phenylacetyl chlorides (B1–B7)

Substituted phenylacetic acid (0.1 mol; **A1–A7**) was taken in a 250 ml dry round bottomed flask. Dry benzene (50–60 ml) was added to it as a solvent. A reflux condenser along with a calcium chloride drying tube and a dropping funnel were attached with the round bottom flask. In the dropping funnel, thionyl chloride (0.4–0.5 mol) was kept and added under anhydrous condition to the substituted phenylacetic acid in a dropwise fashion. After complete addition, the reaction mixture was refluxed for 3–4 h. The reaction was continued until hydrogen chloride (HCl) gas completely evolved out. The end point of the reaction was monitored by thin layer chromatography. Distillation was continued with dry benzene thrice (3 × 50 ml) to remove the excess thionyl chloride to obtain the intended products (**B1–B7**). These compounds (**B1–B7**) were subjected to utilize for the next step of reaction without any purification.

Synthetic procedure of 2-*N*-(substituted phenylacetyl)-L(+)-glutamic acids (C1–C7)

In a dry 250 ml conical flask, L(+)-glutamic acid (0.1 mol) was taken. Glutamic acid was dissolved by adding 2 (N) sodium hydroxide solution slowly to the conical flask so that the reaction mixture became slightly alkaline (pH 8.0). Then the reaction mixture was subjected to continuous stirring on a magnetic stirrer in an ice-salt bath. Small portion of substituted phenylacetyl chlorides (**B1–B7**) were added separately to the alkaline solution from

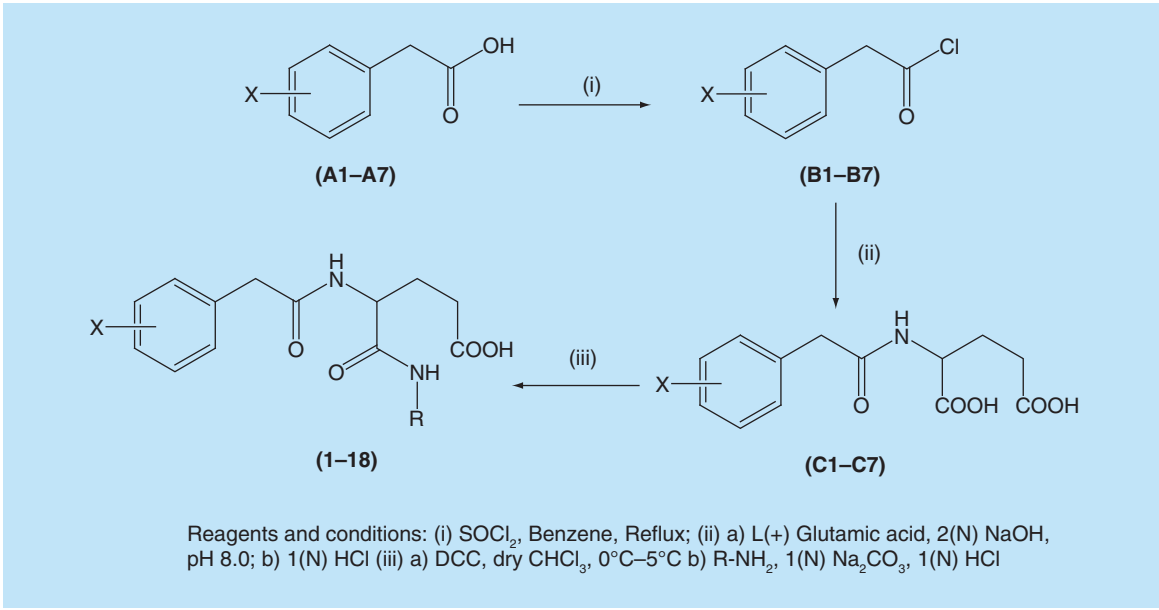

Figure 1. Synthetic route of preparation of substituted pentanoic acid derivatives.

time to time maintaining the alkalinity by addition of 2(N) sodium hydroxide solution with constant stirring. Throughout the reaction, the alkalinity of the reaction mixture was maintained. Thin layer chromatography was utilized to detect completion of the reaction. The unreacted solid products were then filtered off. The clear solution obtained was washed properly with benzene. After discarding the benzene, the aqueous solution is treated with 6(N) hydrochloric acid in cold condition to get the crude solid precipitate. The precipitated crude products were more than 1 h in cold condition for further precipitation. The solid products (**C1–C7**) was filtered off and washed thoroughly with water and dried under vacuum. All these products (**C1–C7**) were recrystallized with hot water and subjected to the next step of reaction.

Synthetic procedure of 1-*N*-substituted-2-*N*-(substituted phenylacetyl)-L(+)-isoglutamines (1–18)

In a 250 ml flat bottom flask, 2-*N*-(substituted phenylacetyl)-L(+) glutamic acid (0.01 mol) was taken dry chloroform (50–60 ml). The *N*,*N*-Dicyclohexyl carbidiimide (DCC; 0.01 mol) was dissolved in dry chloroform (30–40 ml). Slowly, it was added to the reaction mixture with vigorous stirring keeping the system on magnetic stirrer under an ice-salt bath. The stirring was continued for more than 2 h and then amine (0.01 mol) was added to the reaction mixture separately and stirred for more than 6 h. The reaction mixture was kept overnight in a refrigerator. The chloroform layer was separated from the solid dicyclourea (DCU) and the liquid portion was extracted further with 1(N) sodium carbonate (Na_2CO_3) solution. The water layer was separated from the chloroform layer and acidified with 6(N) hydrochloric acid in cold condition and kept in cold for more precipitation. The solid precipitate was filtered separately. It was washed thoroughly with water individually and subsequently dried. The final crude compounds (**1–18**) were recrystallized individually with ethanol. Final compounds **1–18** were characterized by mass, ^{1}H NMR, ^{13}C NMR and FTIR spectroscopy as well as elemental analysis. Mass spectroscopic analysis of these final compounds was done in an LC–MS/MS instrument (the LC, Agilent coupled to electrospray ionization [ESI] mass spectrometer having Mass Hunter Quantitative Analysis software). Nuclear magnetic resonance (NMR) spectra of these final compounds were recorded on AC Bruker 400 MHz FT-NMR spectrometer with tetramethylsilane as the standard internal. ^{13}C NMR of the synthesized compounds was performed by using Bruker 400 MHz FT-NMR spectrometer. Infrared (IR) spectra of these final compounds were performed on a Bruker alpha 11960095 FT-IR instrument. Optical rotation of these derivatives was found in a Perkin-Elmer Type141 polarimeter. PerkinElmer 2400 Series II CHNS/O Elemental Analyzer was used to perform the elemental analyses of these synthesized compounds.

Analytical data of these compounds (**1–18**) are provided below:

(4S)-5-oxo-4-[(phenylacetyl)amino]-5-(butylamino)pentanoic acid (1)

MS (ESI) [M+Na^++H^+] 344.30.^{1}H NMR (DMSO-d6, 300 MHz, ppm) δ 12.25 (s, 1H, COOH), δ 8.39 (d, 1H, CONH, J = 7.36), δ 8.10 (d, 1H, CONH), δ 7.07 (m, 5H, Ar-H), δ 4.41 (m, 1H, CH), δ 3.54 (m, 1H, CH_2), δ 3.20 (s, 2H, CH_2), δ 2.23 (m, 2H, CH_2), δ 2.05 (m, 2H, CH_2), δ 1.54 (m, 2H, CH_2), δ 1.31 (m, 2H, CH_2), δ 0.98 (m, 3H, CH_3). ^{13}C NMR (DMSO-d6, 101 MHz, ppm) δ 174.30, 171.30, 170.55, 136.91, 129.46, 128.60, 126.74, 52.38, 42.49, 38.57, 31.55, 30.60, 28.15, 19.91, 14.10. FTIR (KBr, cm^{-1}): 3286 (NH str of CONH), 3067 (aromatic = C-H str), 2936 (assym. aliphatic CH str), 2882 (sym. aliphatic CH str), 1717 (C=O str COOH), 1634 (C=O str of CONH), 1542 (N-H deformation), 1442 (aliphatic -CH deformation), 1384, 1226 (C-O str and O-H bend of COOH). Anal. Calc. for $C_{17}H_{24}N_2O_4$: C, 63.73; H, 7.55; N, 8.74. Found. C, 63.52; H, 7.82; N, 8.64.

(4S)- (4S)-5-oxo-4-[(phenylacetyl)amino]-5-(isobutylamino)pentanoic acid (2)

MS (ESI) [M+Na^++H^+]: 344.40. ^{1}H NMR (DMSO-d6, 300 MHz, ppm) δ 12.20 (s, 1H, COOH), δ 8.39 (d, 1H, CONH-1, J = 7.36), δ 8.15 (d, 1H, CONH-2), δ 7.07 (m, 5H, Ar-H), δ 4.20 (m, 1H, -CH), δ 3.56 (s, 2H, CH_2), δ 2.20 (m, 2H, CH_2), δ 1.65 (m, 2H, CH_2), δ 1.31, (d, 9H, $3CH_3$). ^{13}C NMR (DMSO-d6, 101 MHz, ppm) δ 174.62, 171.83, 170.72, 136.47, 129.14, 128.38, 126.58, 52.64, 47.62, 38.46, 30.87, 29.84, 27.12, 19.36. FTIR (KBr, cm^{-1}): 3287 (NH str of CONH), 3064 (aromatic = CH str), 2936 (assym. aliphatic -CH str), 2884 (sym. aliphatic -CH str), 1712 (C=O str COOH), 1635 (C=O str of CONH), 1543 (N-H deformation), 1444 (aliphatic –CH deformation), 1390, 1226 (C-O str and O-H bend of COOH). Anal. Calc. for $C_{17}H_{24}N_2O_4$: C, 63.73; H, 7.55; N, 8.74. Found. C, 63.84; H, 7.32; N, 8.53.

(4S)-5-oxo-4-(2-phenylacetamido)-5-(pentylamino)-pentanoic acid (3)

MS (ESI) [M+Na^+]: 357.30. ^{1}H NMR (DMSO-d6, 300 MHz, ppm) δ 12.20 (s, 1H, COOH), δ 8.38 (d, 1H, CONH, J = 7.36), δ 8.12 (d, 1H, CONH), δ 7.05 (m, 5H, Ar-H), δ 4.41 (m, 1H, CH), δ 3.53 (m, 2H, CH_2), δ 3.21 (s, 2H, CH_2), δ 2.24 (m, 2H, CH_2), δ 2.03 (m, 2H, CH_2), δ 1.59 (m, 2H, CH_2), δ 1.31 (m, 4H, $2CH_2$), δ 0.98 (m, 3H, CH_3). ^{13}C NMR (DMSO-d6, 101 MHz, ppm) δ 171.62, 171.43, 170.44, 136.91, 129.48, 128.57, 126.71, 52.82, 42.49, 38.87, 32.31, 29.25, 29.12, 28.96, 22.31, 14.35. FTIR (KBr, cm^{-1}): 3290 (NH str of CONH), 3058 (aromatic = C-H str), 2940 (assym. aliphatic -C-H str), 2882 (sym. aliphatic -CH str), 1726 (C=O str COOH), 1636 (C=O str of CONH), 1545(N-H deformation), 1445 (aliphatic -C-H deformation), 1389, 1224 (C-O str and O-H bend of COOH). Anal. Calc. for $C_{18}H_{26}N_2O_4$: C, 64.65; H, 7.84; N, 8.38. Found. C, 64.54; H, 7.63; N, 8.52.

(S)-5-oxo-4-(2-phenylacetamido)-5-(cyclohexylamino)-pentanoic acid (4)

S (ESI) [M+Na^+]: 369.01. ^{1}H NMR (DMSO-d6, 300 MHz, ppm) δ 8.39 (d, 1H, CONH, J = 7.36), δ 8.15 (d, 1H, CONH), δ 7.18 (m, 5H, Ar-H), δ 4.52 (m, 1H, CH), δ 3.69 (s, 2H, -CH), δ 3.54 (m, 2H, CH_2), δ 3.48 (m, 1H, CH), δ 2.07 (m, 2H, CH_2), δ 1.68 (m, 2H, CH_2), 1.31 (m, 10H, c-Hex). ^{13}C NMR (DMSO-d6, 101 MHz, ppm) δ 173.45, 171.62, 170.39, 136.64, 129.72, 128.54, 126.41, 52.72, 46.36, 32.18, 32.02, 30.42, 27.62, 25.87, 24.32, 24.13. FTIR (KBr, cm^{-1}): 3291 (N-H str of CONH), 3055 (aromatic = CH str), 2936 (assym. aliphatic -CH str), 2880 (sym. aliphatic -CH str), 1725 (C=O str COOH), 1637 (C=O str of CONH), 1543 (N-H deformation), 1447 (aliphatic –CH deformation), 1412 (C-O str of COOH), 1173 (O-H str of COOH). Anal. Calc. for $C_{19}H_{26}N_2O_4$: C, 65.87; H, 7.56; N, 8.09. Found. C, 65.98; H, 7.65; N, 8.22.

(S)-5-oxo-4-(2-phenylacetamido)-5-(phenylamino)-pentanoic acid (5)

MS (ESI) [M+Na^+]: 363.14. ^{1}H NMR (DMSO-d6, 300 MHz, δ ppm) δ 12.18 (s, 1H, COOH), δ 10.10 (s, 1H, CONH), δ 8.42 (d, 1H, CONH, J = 7.74), δ 7.06 (m, 10H, Benzene), δ 4.53 (m, 1H, CH), δ 3.44 (s, 2H, CH_2), δ 2.26 (m, 2H, CH_2), δ 2.01 (m, 2H, CH_2). ^{13}C NMR (DMSO-d6, 101 MHz, ppm) δ 174.42, 171.26, 170.58, 140.78, 136.41, 129.22, 128.42, 127.54, 126.41, 124.87, 120.87, 52.42, 40.23, 30.42, 27.12. FTIR (KBr, cm^{-1}): 3321 (N-H str of CONH), 3075 (aromatic = CH str), 2935 (assym. aliphatic -C-H str), 2867 (sym. aliphatic -CH str), 1726 (C=O str COOH), 1612 (aromatic C=C str), 1541 (N-H deformation), 1449 (aliphatic -C-H deformation), 1416, 1245 (C-O str and O-H bend of COOH). Anal. Calc. for $C_{19}H_{20}N_2O_4$: C, 67.05; H, 5.92; N, 8.23. Found. C, 67.23; H, 5.84; N, 8.37.

(4S)-4-{[(2-methylphenyl)acetyl]amino}-5-oxo-5-(phenylamino)pentanoic acid (6)

MS (ESI) [M+Na^+]: 377.10. ^{1}H NMR (DMSO-d6, 300 MHz, δ ppm) δ 12.25 (s, 1H, COOH), δ 10.14 (s, 1H, CONH), δ 8.42 (d, 1H, CONH, J = 7.74), δ 7.06 (m, 10H, Ar-H), δ 4.53 (m, 1H, CH), δ 3.44 (s, 2H, CH_2), δ 2.21 (s, 3H, CH_3), δ 2.10 (m, 2H, CH_2), δ 2.02 (m, 2H, CH_2). ^{13}C NMR (DMSO-d6, 101 MHz, ppm) δ 174.62, 171.38, 170.40, 140.90, 139.23, 136.72, 129.62, 128.24, 127.82, 126.10, 124.42, 120.70, 52.65, 33.47, 30.11, 27.26, 14.74. FTIR (KBr, cm-1): 3350 (N-Hstr of CONH), 3069 (aromatic = CH str), 2934 (assym. aliphatic -CH str), 2869 (sym. aliphatic -CH str), 1725 (C=O str COOH), 1611 (aromatic C=C str), 1547 (NH deformation), 1447 (aliphatic –CH deformation), 1415, 1246 (C-O str and O-H bend of COOH). Anal. Calc. for $C_{20}H_{22}N_2O_4$: C, 67.78; H, 6.26; N, 7.90. Found. C, 67.54; H, 6.35; N, 7.98.

(4S)-4-{[(2-fluorophenyl)acetyl]amino}-5-oxo-5-(propylamino)pentanoic acid (7)

MS (ESI) [M+Na^+]: 347.10. ^{1}H NMR (300 MHz, DMSO-d6, ppm): δ 12.16 (s, 1H, COOH), δ 8.13 (d, 1H, CONH-2, J = 8.07), δ 7.84 (m, 1H, CONH-1), δ 7.17 (m, 5H, Ar-H), δ 4.14 (m, 1H, CH), δ 3.56 (s, 2H, CH_2), δ 3.28 (s, 2H, CH_2), δ 2.21 (m, 2H, CH_2), δ 1.99 (m, 2H, CH_2), δ 1.51 (m, 2H, CH2), δ 0.96 (m, 3H, CH_3). ^{13}C NMR (DMSO-d6, 101 MHz, ppm) δ 174.41, 170.62, 169.54, 162.81, 132.62, 129.18, 124.72, 123.65, 115.98, 52.40, 42.98, 29.87, 27.50, 28.42, 24.61. FTIR (KBr, cm^{-1}): 3309 (N-H str of CONH), 3105 (aromatic = C-H str), 2961 (assym. aliphatic –CH_3 str), 2932 (assym. aliphatic -CH2 str), 2874 (sym. aliphatic –CH_3 str), 1727 (C=O str COOH), 1648 (C=O str of CONH), 1612 (aromatic C=C str), 1544 (N-H deformation of CONH), 1496 (aliphatic -CH_2 deformation), 1446 (aliphatic –CH_3 deformation), 1415, 1231 (C-O str and O-H bend of COOH), 1172 (aromatic C-F str), 1032 (aromatic = C-H in plane deformation), 957 (O-H out of plane deformation of COOH). Anal. Calc. for $C_{16}H_{21}N_2O_4F$: C, 59.25; H, 6.53; N, 8.64. Found. C, 59.02; H, 6.67; N, 8.52.

(4S)-4-{[(2-fluorophenyl)acetyl]amino}-5-oxo-5-(isopropylamino)pentanoic acid (8)

MS (ESI) [M+Na^+]: 347.10. ^{1}H NMR (300 MHz, DMSO-d6, ppm): δ 12.11 (s, 1H, COOH), δ 8.20 (d, 1H, CONH-2, J = 8.07), δ 7.85 (m, 1H, CONH-1), δ 7.10 (m, 5H, Benzene), δ 4.19 (m, 1H, CH), δ 3.40 (s, 2H, CH_2), δ 2.12 (m, 2H, CH_2), δ 1.73-1.83 (m, 2H, CH_2), δ 0.98 (d, 6H, $2CH_3$). ^{13}C NMR (DMSO-d6, 101 MHz, ppm) δ 174.33, 170.38, 169.49, 162.25, 132.21, 129.02, 124.58, 123.92, 115.51, 52.36, 40.86, 35.52, 30.58, 28.28, 22.76. FTIR (KBr, cm^{-1}): 3309 (N-H str of CONH), 3105 (aromatic = C-H str), 2961 (assym. aliphatic –CH_3 str), 2932 (assym. aliphatic -CH_2 str), 2876 (sym. aliphatic –CH_3 str), 1724 (C=O str COOH), 1641 (C=O str of CONH), 1615 (aromatic C = C str), 1547 (N-H deformation of CONH), 1496 (aliphatic -CH_2 deformation), 1446 (aliphatic –CH_3 deformation), 1417, 1231 (C-O str and O-H bend of COOH), 1170 (aromatic C-F str), 1044 (aromatic = C-H in plane deformation), 964 (O-H out of plane deformation of COOH). Anal. Calc. for $C_{16}H_{21}N_2O_4F$: C, 59.25; H, 6.53; N, 8.64. Found. C, 59.18; H, 6.48; N, 8.72.

(4S)-4-{[(2-fluorophenyl)acetyl]amino}-5-oxo-5-(isobutylamino)pentanoic acid (9)

MS (ESI) [M+Na^+]: 361.15. ^{1}H NMR (300 MHz, DMSO-d6, ppm): δ 12.11 (s, 1H, COOH), δ 8.20 (d, 1H, CONH-2, J = 8.07), δ 7.85 (m, 1H, CONH-1), δ 7.10 (m, 5H, Benzene), δ 4.19 (m, 1H, CH), δ 3.56 (s, 2H, CH_2), δ 2.80 (m, 2H, CH_2), δ 2.15 (m, 2H, CH_2), δ 1.80 and 1.67 (m, 2H, CH_2), δ 1.63 (m, 1H, CH), δ 0.84 (d, 6H, $2CH_3$). ^{13}C NMR (DMSO-d6, 101 MHz, ppm) δ 174.31, 170.62, 169.24, 162.32, 132.46, 128.98, 124.74, 123.76, 116.42, 52.39, 49.53, 30.48, 29.91, 28.41, 26.43, 19.45. FTIR (KBr, cm^{-1}): 3309 (N-H str of CONH), 3100 (aromatic = C-H str), 2963 (assym. aliphatic –CH_3 str), 2927 (assym. aliphatic -CH_2 str), 2884 (sym. aliphatic – CH_3 str), 1730 (C=O str COOH), 1652 (C=O str of CONH), 1612 (aromatic C=C str), 1547 (N-H deformation of CONH), 1450 (aliphatic –CH_3 deformation), 1418, 1230 (C-O str and O-H bend of COOH), 1178 (aromatic C-F str), 1031 (aromatic = C-H in plane deformation), 955 (O-H out of plane deformation of COOH). Anal. Calc. for $C_{17}H_{23}N_2O_4F$: C, 60.34; H, 6.85; N, 8.28. Found. C, 60.46; H, 6.93; N, 8.16.

(4S)-4-{[(2-chlorophenyl)acetyl]amino}-5-oxo-5-(butylamino)pentanoic acid (10)

MS (ESI) [M+Na^++H^+]: 377.12, ^{1}H NMR (300 MHz, DMSO-d6, ppm): δ 12.11 (s, 1H, COOH), δ 8.20 (d, 1H, CONH, J = 8.01), δ 7.86 (m, 1H, CONH), δ 7.23 (m, 4H, Ar-H), δ 4.19 (m, 1H, CH), δ 3.55 (s, 2H, CH_2), δ 3.02 (m, 2H, CH_2), δ 2.18 (m, 2H, CH_2), δ 1.72 (m, 2H, CH2), δ 1.32 (m, 2H, CH_2), δ 1.29 (m, 2H, CH_2), δ 0.84-0.88 (m, 3H, CH_3). ^{13}C NMR (DMSO-d6, 101 MHz, ppm) δ 173.82, 170.46, 169.30, 136.28, 135.43, 131.28, 129.67, 128.32, 127.22, 52.74, 42.68, 33.81, 30.41, 29.80, 27.32, 20.4, 13.87. FTIR (KBr, cm^{-1}): 3310

(N-H str of CONH), 3062 (aromatic = C-H str), 2944 (assym. aliphatic -CH str), 2877 (sym. aliphatic -C–H str), 1725 (C=O str COOH), 1650 (C=O str of CONH), 1615 (aromatic C=C str), 1540 (N-H deformation), 1442 (aliphatic -C-H deformation), 1415, 1263 (C-O str and O-H bend of COOH). Anal. Calc. for $C_{17}H_{23}N_2O_4Cl$: C, 57.54; H, 6.53; N, 7.89. Found. C, 57.62; H, 6.66; N, 7.78.

(4S)-4-{[(2-chlorophenyl)acetyl]amino}-5-oxo-5-(hexylamino)pentanoic acid (11)

MS (ESI): $[M+Na^+]$: 404.10, ^1H NMR (300 MHz, DMSO-d6, δ ppm): δ 12.11 (s, 1H, COOH), δ 8.20(d, 1H, CONH, J = 8.01), δ 7.86 (m, 1H, CONH), δ 7.23 (m, 4H, Ar-H), δ 4.14 (m, 1H-2, CH), δ 3.30 (s, 2H, CH_2), δ 2.95 (m, 2H, CH_2), δ 2.07 (m, 2H, CH_2), δ 1.69 (m, 2H, CH_2), δ 1.32 (m, 2H, CH_2), δ 1.22 (m, 3H, $3CH_2$), δ 0.89 (m, 3H, CH_3). ^{13}C NMR (DMSO-d6, 101 MHz, ppm) δ 173.61, 170.48, 169.89, 136.41, 135.63, 131.32, 129.10, 128.32, 127.43, 52.69, 42.76, 32.30, 31.84, 29.12, 27.42, 27.14 22.68, 14.63. FTIR (KBr, cm^{-1}): 3315 (N-H str of CONH), 3064 (aromatic = C-H str), 2944 (assym. aliphatic -C-H str), 2879 (sym. aliphatic -C–H str), 1724 (C=O str COOH), 1647 (C=O str of CONH), 1616 (aromatic C=C str), 1548 (N-H deformation), 1443 (aliphatic -C-H deformation), 1415, 1263 (C-O str and O-H bend of COOH). Anal. Calc. for $C_{19}H_{27}N_2O_4Cl$: C, 59.60; H, 7.11; N, 7.32. Found. C, 59.48; H, 7.23; N, 7.17.

(4S)-4-{[(4-methoxyphenyl)acetyl]amino}-5-oxo-5-(t-butylamino)pentanoic acid (12)

MS (ESI) $[M+Na^+]$ 373.21.^1H NMR (DMSO-d6, 300 MHz, ppm) δ 12.20 (s, 1H, COOH), δ 8.39 (d, 1H, CONH, J = 7.36), δ 8.15 (d, 1H, CONH), δ 7.07 (m, 5H, Ar-H), δ 4.20 (m, 1H, CH), δ 3.70 (s, 3H, CH_3), δ 3.52 (s, 2H, CH_2), δ 2.24 (m, 2H, CH_2), δ 1.72 (m, 2H, CH_2), δ1.34 (d, 9H, $3CH_3$). ^{13}C NMR (DMSO-d6, 101 MHz, ppm) d 172.74, 170.26, 149.82, 147.19, 128.54, 124.75, 55.83, 40.66, 31.51, 28.34, 22.76. FTIR (KBr, cm^{-1}): 3321 (NH str of CONH), 3065 (aromatic = CH str), 2940 (assym. aliphatic -C-H str), 2890 (sym. aliphatic –CH str), 1717 (C=O str COOH), 1636 (C=O str of CONH), 1543 (N-H deformation), 1442 (aliphatic -CH deformation), 1392, 1229 (C-O str and O-H bend of COOH). Anal. Calc. for $C_{18}H_{26}N_2O_5$: C, 61.70; H, 7.48; N, 7.99. Found. C, 61.84; H, 7.35; N, 8.06.

(4S)-4-{[(4-bromophenyl)acetyl]amino}-5-oxo-5-(propylamino)pentanoic acid (13)

MS (ESI) $[M+Na^+]$: 408.12. ^1H NMR (300 MHz, DMSO-d6, ppm): δ 12.10 (s, 1H, COOH), δ 8.28 (d, 1H, CONH-2, J = 8.13), δ 7.76 (m, 1H, CONH-1), δ 7.47 (m, 2H-3', 5'- Benzene), δ 7.19 (m, 2H-2', 6'Benzene), δ 4.16 (m, 1H-2, CH), δ 3.30 (s, 2H-1', CH_2), δ 3.57 (m, 1H-1", $-CH_2$), δ 3.28 (s, 2H-1', $-CH_2$), δ 2.21 (m, 2H-4, $-CH_2$), δ 1.99 (m, 2H- 3, $-CH_2$), δ 1.51 (m, 2H-2", $-CH_2$), δ 0.96 (m, 3H-3", $-CH_3$). ^{13}C NMR (DMSO-d6, 101 MHz, ppm) δ 173.77, 170.80, 169.62, 135.83, 131.25, 130.94, 119.47, 51.93, 41.21, 40.21, 30.11, 27.65, 22.21, 11.25. FTIR (KBr, cm^{-1}): 3292(N-H str of CONH), 3097 (aromatic = C-H str), 2928 (assym. aliphatic -C-H str), 2856 (sym. aliphatic -C–H str), 1712 (C=O str COOH), 1647 (C=O str of CONH), 1634 (aromatic C=C str), 1546 (N-H deformation), 1488 (aliphatic -C-H deformation), 1408, 1228 (C-O str and O-H bend of COOH). Anal. Calc. for $C_{16}H_{21}N_2O_4Br$: C, 49.88; H, 5.49; N, 7.27. Found. C, 49.73; H, 5.56; N, 7.18.

(4S)-4-{[(4-bromophenyl)acetyl]amino}-5-oxo-5-(butylamino)pentanoic acid (14)

MS (ESI) $[M+Na^+]$: 420.12. ^1H NMR (300 MHz, DMSO-d6, ppm): δ 12.11 (s, 1H, COOH), δ 8.20-8.34 (d, 1H, CONH, J = 8.13), δ 7.75 (m, 1H, CONH), δ 7.44 (m, 2H, Ar- H), δ 7.18(m, 2H, Ar-H), δ 4.19 (m, 1H, CH), δ 3.55 (s, 2H, CH_2), δ 3.02 (m, 2H, CH_2), δ 2.18 (m, 2H, CH_2), δ 1.70 (m, 2H, $-CH_2$), δ 1.32 (m, 2H, CH_2), δ 1.22 (m, 2H, CH_2), δ 0.84 (m, 3H, CH_3). ^{13}C NMR (DMSO-d6, 101 MHz, ppm) δ 173.58, 170.72, 169.81, 135.61, 131.38, 130.84, 120.46, 52.36, 41.46, 40.08, 33.96, 30.42, 27.84, 22.74, 11.64. FTIR (KBr, cm^{-1}): 3309 (N-H str of CONH), 3105 (aromatic = C-H str), 2932 (assym. aliphatic -C-H str), 2874 (sym. aliphatic -C–H str), 1727 (C=O str COOH), 1648 (C=O str of CONH), 1612 (aromatic C=C str), 1544 (N-H deformation), 1415, 1231 (C-O str and O-H bend of COOH). Anal. Calc. for $C_{17}H_{23}N_2O_4Br$: C, 51.14; H, 5.81; N, 7.02. Found. C, 51.23; H, 5.69; N, 7.14.

(4S)-4-{[(4-bromophenyl)acetyl]amino}-5-oxo-5-(isobutylamino)pentanoic acid (15)

MS (ESI) $[M+Na^+]$: 420.12, ^1H NMR (300 MHz, DMSO-d6, ppm): δ 12.11 (s, 1H, COOH), δ 8.20-8.34 (d, 1H, CONH, J = 8.13), δ 7.75 (m, 1H, CONH), δ 7.44-7.47 (m, 2H, Ar-H), δ 7.18 (m, 2H, Ar-H), δ 4.22 (m, 1H, CH), δ 3.57 (s, 2H, CH_2), δ 2.82 (m, 2H, CH_2), δ 2.19 (m, 2H, CH_2), δ 1.63 (m, 2H, CH_2), δ 0.79, (d, 7H, $CH(CH_3)_2$). ^{13}C NMR (DMSO-d6, 101 MHz, ppm) δ 178.62, 174.53, 170.54, 135.24, 132.34, 132.12,

120.37, 52.68, 48.53, 39.24, 31.24, 29.84, 27.32, 18.63. FTIR (KBr, cm^{-1}): 3312 (NH str of CONH), 3110 (aromatic = C-H str), 2933 (assym. aliphatic -C-H str), 2876 (sym. aliphatic -C–H str), 1724 (C=O str COOH), 1649 (C=O str of CONH), 1612 (aromatic C=C str), 1544 (N-H deformation), 1415, 1231 (C-O str and O-H bend of COOH). Anal. Calc. for $C_{17}H_{23}N_2O_4Br$: C, 51.14; H, 5.81; N, 7.02. Found. C, 51.22; H, 5.92; N, 7.18.

(4S)-4-{[(4-bromophenyl)acetyl]amino}-5-oxo-5-(cyclohexylamino)pentanoic acid (16)

MS (ESI) $[M+Na^+]$: 447.07, ^1H NMR (300 MHz, DMSO-d6, ppm): δ 12.11 (s, 1H, COOH), δ 8.20-8.34 (d, 1H, CONH-2, J = 8.13), δ 7.75-7.87 (m, 1H, CONH-1), δ 7.44- 7.47 (m, 2H, Ar-H), δ 7.18 (m, 2H, Ar-H), δ 4.14 (m, 1H, CH), δ 3.69 (s, 2H, CH_2), δ 3.54 (m, 2H-1, CH_2), δ 2.07 (m, 2H-4, CH_2), δ 1.68 (m, 2H-3, CH_2), δ 1.26 (m, 10H, c-Hex). ^{13}C NMR (DMSO-d6, 101 MHz, ppm) δ 173.80, 169.86, 169.59, 135.84, 131.23, 130.96, 119.49, 51.81, 47.36, 41.24, 32.26, 32.10, 30.13, 27.85, 25.13, 24.41, 24.35. FTIR (KBr, cm^{-1}): 3292 (N-H str of CONH), 3097 (aromatic = C-H str), 2929 (assym. aliphatic -C-H str), 2858 (sym. aliphatic -C–H str), 1718 (C=O str COOH), 1649 (C=O str of CONH), 1639 (aromatic C=C str), 1546 (N-H deformation), 1487 (aliphatic -C-H deformation), 1408, 1228 (C-O str and O-H bend of COOH). Anal. Calc. for $C_{19}H_{25}N_2O_4Br$: C, 53.65; H, 5.92; N, 6.59. Found. C, 53.78; H, 6.02; N, 6.48.

(4S)-4-{[(4-chlorophenyl)acetyl]amino}-5-oxo-5-(propylamino)pentanoic acid (17)

MS (ESI) $[M+Na^+]$: 363.10. ^1H NMR (300 MHz, DMSO-d6, ppm): δ 12.07 (s, 1H, COOH), δ 8.43 (m, 1H, CONH), δ 8.28 (d, 1H, CONH, J = 8.31), δ 7.18 (m, 5H, Ar-H), δ 4.42 (m, 1H, CH), δ 3.54 (m, 1H, CH_2), δ 3.28 (s, 2H, CH_2), δ 2.21 (m, 2H, CH_2), δ 1.99 (m, 2H, CH_2), δ 1.51 (m, 2H, CH_2), δ 0.96 (m, 3H, CH_3). ^{13}C NMR (DMSO-d6, 101 MHz, ppm) δ 178.78, 172.65, 169.48, 134.56, 132.80, 131.32, 130.96, 51.45, 47.24, 39.42, 37.32, 25.84, 24.87, 11.78. FTIR (KBr, cm^{-1}): 3309 (NH str of CONH), 3063 (aromatic = C-H str), 2942 (assym. aliphatic -C-H str), 2877 (sym. aliphatic -CH str), 1727 (C=O str COOH), 1647 (C=O str of CONH), 1604 (aromatic C=C str), 1542 (N-H deformation), 1439 (aliphatic -CH deformation), 1411, 1261 (C-O str and O-H bend of COOH), 966 (O-H out of plane deformation of COOH), 806, 750, 696, 651 (aromatic –C-H out of plane deformation). Anal. Calc. for $C_{16}H_{21}N_2O_4Cl$: C, 56.39; H, 6.21; N, 8.22. Found. C, 56.46; H, 6.32; N, 8.13.

(4S)-4-{[(4-chlorophenyl)acetyl]amino}-5-oxo-5-(isopropylamino)pentanoic acid (18)

MS (ESI) $[M+Na^+]$: 363.20. ^1H NMR (300 MHz, DMSO-d6, ppm): δ 12.08 (s, 1H, COOH), δ 8.46 (m, 1H, CONH), δ 8.30 (d, 1H, CONH, J = 8.30), δ 7.16 (m, 5H, Benzene), δ 4.18 (m, 1H, CH), δ 3.84 (m, 1H, CH_2), δ 3.48 (s, 2H, CH_2), δ 2.15 (m, 2H, CH_2), δ 1.73 (m, 2H, CH_2), δ 0.95 (d, 6H, $2CH_3$). ^{13}C NMR (DMSO-d6, 101 MHz, ppm) δ 178.42, 173.68, 169.54, 134.81, 132.24, 131.422, 129.64, 52.84, 43.57, 38.62, 29.45, 27.64, 23.64. FTIR (KBr, cm^{-1}): 3310 (NH str of CONH), 3060 (aromatic = C-H str), 2930 (assym. aliphatic CH str), 2874 (sym. aliphatic -C–H str), 1726 (C=O str COOH), 1648 (C=O str of CONH), 1610 (aromatic C=C str), 1541 (N-H deformation), 1434 (aliphatic -C-H deformation), 1409, 1263 (C-O str and O-H bend of COOH). Anal. Calc. for $C_{16}H_{21}N_2O_4Cl$: C, 56.39; H, 6.21; N, 8.22. Found. C, 56.28; H, 6.28; N, 8.31.

Biological screening

Cell lines

Human cancer cell lines U937 (acute myeloid leukemia), Jurkat-E6.1 (T-acute lymphocytic leukemia; T-ALL), MOLT-4 (T-ALL), MCF-7 and MDA-MB-231 (Breast cancer), HepG2 (liver cancer) and HUT-78 (lymphoma) were obtained from National Centre for Cell Science (NCCS), Pune, India. Human peripheral blood mononuclear cells (PBMC) were collected from a healthy volunteer. All these cell lines except MDA-MB-231 were cultured in RPMI-1640 media with 10% FBS and 1% antibiotic. MDA-MB-231 was cultured in Dulbecco's modified Eagle medium media with 10% FBS and 1% antibiotic. These cells were maintained in 37°C with 5% CO_2 in humified incubator. 0.025% Trypsin in saline was used for harvesting adherent cells.

Treatment with the synthesized compounds

These cells suspended separately in media and were plated and kept in the 37°C incubator for 20 h. Then treatments were given with these synthesized compounds diluted in saline at different concentrations. After adding these compounds at desired concentrations, cells were incubated in the incubator for 40–48 h before any experiment.

Cytotoxicity assay

To determine the cytotoxicity, cells were seeded in 96 well plate at a concentration of 1×10^3 per well. The cells were allowed to settle for 24 h in an incubator. Then treatment was given with these compounds individually at different concentration for 48 h in the incubator. MTT was added at a concentration of 1 mg/ml and incubation was done for 4 h. DMSO was added to stop the reaction and absorbance was measured at 570 nm in microplate photometer (Thermo Scientific Multiscan FC; MA USA). The control value of untreated cells was taken as 100% and the treated cells cytotoxicity was calculated as the percentage of the control.

Apoptotic assay by flow cytometry after annexin V/ PI staining

Jurkat-E6.1 cells were plated at a cell number of 5×10^4. After 24 h, treatment was given with **31** (2 μM, 5 μM) and **18** (10 μM, 20 μM). 48 hours post treatment, these cells were centrifuged in 15 ml tube and then washed with saline. Then the washed cells were treated with annexin V-FITC (100 ng/ml) and propidium iodide (PI; 50 μg/ml) and were incubated in the dark at room temperature for 15 min. Finally apoptosis was analyzed by flow cytometry (FACS BD Fortessa) [3,36].

Mitochondrial membrane potential analysis

JC-1 is a lipophilic cationic dye which was used to measure mitochondrial transmembrane potential ($\Delta\Psi m$) [37]. Jurkat-E6.1 cells were plated in 6-well plate at a number of 1×10^5 cells per well and these cells were incubated for 24 h in CO_2 incubator at 37°C. After incubation treatment was given with **18** (10 μM, 20 μM) and **31** (2 μM, 5 μM). 48 hours post treatment, these cells were harvested and washed with saline. The washed cells were then treated with JC1dye and these treated cells were incubated in dark for 25 min. After 25 min, these cells were washed with saline. The washed cells were finally resuspended in saline and flow cytometry analysis was done in BD FACS AriaII cell sorter. An excitation wavelength of 488 nm and emission wavelength of 530 nm were used for green and that of 590 nm was used for red fluorescence. The membrane potential was analyzed by FACSDIVA software (BD Biosciences; CA, USA).

MMP-2 & HDAC8 expression analysis

Jurkat-E6.1 cells were plated (5×10^4). After 24 h, treatment was given with **31** (2 μM, 5 μM) and **18** (10 μM, 20 μM). 48 hours post treatment these treated cells were centrifuged at 1200 rpm for 10 min in 15 ml tube and the cell pellet was washed with saline. Then 70% chilled ethanol was added to the cells and these cells were incubated in ethanol for 1 h. After 1 h cells were washed with saline and incubated in blocking solution containing 5% FBS and 0.02% Tween 80 in saline, for 1 h at room temperature. After blocking, these cells were washed with saline and treated with anti MMP-2 and anti HDAC-8 primary antibody (1:250) in two different sets overnight. After incubation the cells were washed with saline. The washed cells were then treated with secondary antibody conjugated with FITC (1:250) for 1 h. After treatment with secondary antibody the cells were washed with saline and the expression of MMP-2 and HDAC-8 were analyzed by flow cytometry (FACS BD Fortesa).

DNA nick generation

Jurkat-E6.1 cells (1×10^5) were plated in 6-well plate and allowed to grow for 24 h. Treatment was given with **31** (2 μM and 5 μM) and again incubated for 48 h [36]. The treated cells were washed and for fixing the cells were incubated overnight with 70% chilled ethanol. After fixation cells were washed twice with saline. Then 10 μM DAPI stain was added to the cell and incubated in dark for 30 min. After incubation cells were mounted on a clean glass slide and seen under fluorescence microscope (Ziess Axiovert 40CFL).

Cell cycle analysis

Jurkat-E6.1 cells were plated at a number of 5×10^4 cell per well. Plated cells were treated with **31** at a concentration of 2 and 5 μM for 48 h. Then cells were centrifuged and washed with saline. Then these cells were fixed with 70% chilled ethanol overnight. After fixation the cells were washed with saline twice. The washed cells then was treated with RNAse (100 ng/ml) for 1 h. at room temperature [36]. Then 50 μg/ml PI was added and incubated for 15 min in the dark and was analyzed by flow cytometry (FACS BD Fortessa).

Binding mode interaction studies

Molecular docking study of the best active pentanoic acids among the newly synthesized (**18**) and earlier synthesized (**31**) compounds with these metalloenzymes was carried out following the same protocol reported earlier [3,36,38,39] using Maestro software of Schrodinger Inc. USA [40].

Statistical analysis

All these results reported were the arithmetic mean of the data. Independent experiments were performed in triplicate. Each group was having six in number. Results were shown as mean ± standard deviation (SD). Statistical analysis was done by one-way analysis of variance (ANOVA) having LSD *post-hoc* test using SPSS 16 software. Statistical significance was $p \leq 0.001$.

Results & discussion

Synthesis

The substituted phenylacetic acids (**A1–A7**) were converted individually to prepare the corresponding acid chlorides (**B1–B7**) by refluxing with thionyl chloride in presence of dry benzene. Acid chlorides (**B1–B7**) were subjected to the next step without further purification. These acid chlorides (**B1–B7**) were condensed with L(+)glutamic acid at slightly alkaline condition (pH 8.0) to obtain substituted phenylacetyl L(+) glutamic acids (**C1–C7**). These diacids (**C1–C7**) were recrystalized separately with dilute ethanol and subjected to the next step of reaction. The diacid compounds **C1–C7** were stirred in DCC in the presence of dry chloroform on an icebath for overnight and then were treated individually with various amines for more than 12 hr. The solid products were removed separately through filtration and the organic layers were extracted with 1(N) sodium carbonate. The aqueous layers were acidified individually with 1(N) hydrochloric acid dropwise in an ice bath to get the desired final compounds (**1–18**). Completion of each step of reaction was monitored by thin layer chromatography. The final compounds (**1–18**) were recrystallized with hot ethanol. Purity of these compounds was determined by ^{1}H NMR, ^{13}C NMR, mass and IR spectroscopic and elemental analyses. Positive optical activity was obtained when all synthesized compounds (**1–18**) were placed seperately in a Perkin–Elemer type 141 polarimeter. Physical properties of these compounds are provided in Table 1.

Biological screening

These synthesized compounds (**1–18**) were preliminary screened for cytotoxic evaluation against a panel of cancer cell lines such as U937, Jurkat-E6.1, MOLT-4, MDA-MB-231, MCF-7, HEPG-2 and HUT-78 as well as their effects in normal cell: PBMC. Apart from these compounds, another 17 earlier reported molecules (**19–35**) [3] were taken into consideration to judge their efficacy against these cell lines. The potential lead molecules were further evaluated for apoptotic assay, mitochondrial membrane potential assay, DNA nick generation assay and cell cycle analysis in Jurkat-E6.1 cell line. Nevertheless, flow cytometric analysis of these potential lead molecules were also performed in Jurkat-E6.1 cells to observe the change in MMP-2 and HDAC8 expression levels.

Cytotoxicity study

In order to determine the cytotoxicity of compounds **1–18**, the MTT assay was performed in a variety of cancer cell lines (leukemia: Jurkat-E6.1, MOLT 4, U937; breast cancer: MDA-MB-231, MCF-7; T-cell lymphoma: HUT-78; liver cancer: HEPG2) along with normal cells-PBMC [3,36]. These cancer cell lines and PBMC were treated with the synthesized compounds **1–18** and MTT was added that produced crystal violet farmazan in the presence of DMSO in live cells. The absorbance of the crystal violet coloration decreased gradually which indicated death of the treated cells. It was interesting to note that all these compounds were inactive against PBMC and showed very poor cytotoxicity for solid tumor breast cancer cell lines MDA-MB-231 and MCF-7 along with lymphoma cell line HUT 78 as well as liver cancer cell line HEPG2 (Table 2). However, these compounds produced moderate to good cytotoxicity in T-acute lymphocytic leukemia (T-ALL) cell lines namely Jurkat-E6.1 and MOLT-4. Again, these compounds were found to exert cytotoxicity against acute myeloid leukemia cell line U937. Besides these, cytotoxic potential of 17 earlier reported compounds (**19–35**) [3] was also evaluated. These are also shown in Table 2.

Compound **18** of the current series of newly synthesized molecules was the most cytotoxic against Jurkat-E6.1 and MOLT-4 cell lines. However, **31** among all compounds (both newly synthesized and earlier reported molecules) showed the highest activity in these entire leukemia cell lines (U937, Jurkat-E6.1 and MOLT-4). Selectivity of

10.4155/fmc-2018-0361

Table 1. Physicochemical parameters of the final compounds (1–18).

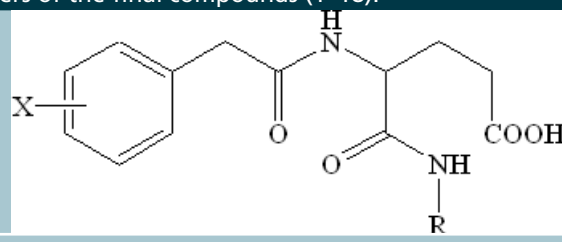

Compound†	X	R	Molecular formula	MW	Yield (%)	MP (°C)
1	H	*n*-But	$C_{17}H_{24}N_2O_4$	320.38	64	148–150
2	H	*i*-But	$C_{17}H_{24}N_2O_4$	320.38	56	170–172
3	H	*n*-Pent	$C_{18}H_{26}N_2O_4$	334.41	58	124–126
4	H	*c*-Hex	$C_{19}H_{26}N_2O_4$	346.42	48	166–168
5	H	Ph	$C_{19}H_{20}N_2O_4$	340.37	39	188–190
6	2-Me	Ph	$C_{20}H_{22}N_2O_4$	354.40	45	216–218
7	2-F	*n*-Pr	$C_{16}H_{21}FN_2O_4$	324.35	20	204–206
8	2-F	*i*-Pr	$C_{16}H_{21}FN_2O_4$	324.35	36	228–230
9	2-F	*i*-But	$C_{17}H_{23}FN_2O_4$	338.37	71	202–204
10	2-Cl	*n*-But	$C_{17}H_{23}ClN_2O_4$	354.83	58	192–194
11	2-Cl	*n*-Hex	$C_{19}H_{27}ClN_2O_4$	382.88	77	153–155
12	4-OMe	*t*-But	$C_{18}H_{26}N_2O_5$	350.41	65	125–127
13	4-Br	*n*-Pr	$C_{16}H_{21}BrN_2O_4$	385.25	47	147–150
14	4-Br	*n*-But	$C_{17}H_{23}BrN_2O_4$	399.28	39	146–148
15	4-Br	*i*-But	$C_{17}H_{23}BrN_2O_4$	399.28	35	148–150
16	4-Br	*c*-Hex	$C_{19}H_{25}BrN_2O_4$	425.32	46	188–190
17	4-Cl	*n*-Pr	$C_{16}H_{21}ClN_2O_4$	340.80	18	154–156
18	4-Cl	*i*-Pr	$C_{16}H_{21}ClN_2O_4$	340.80	48	140–142

MP: Melting point; MW: Molecular weight.

these compounds (index of selectivity) between normal cell PBMC and cancer cells (such as Jurkat-E6.1, U937 and MOLT-4) was determined [41] and presented in Table 3.

It is clearly observed that all these compounds were cytotoxic and but nontoxic over PBMC cell lines as suggested by their selectivity indices.

Apoptotic assay

The route of cell death whether by apoptosis or necrosis was confirmed by this study. This study was done by flow cytometric analysis after dual staining of the Jurkat-E6.1 cells with annexin V and PI [3,36]. Here, annexinV/PI negative cells indicate early apoptosis and annexin V/ PI positive cells indicate late apoptosis. As **18** and **31** resulted in the best cytotoxicity among these synthesized compounds and earlier reported molecules [3], these two compounds were further subjected to apoptotic study. **18** showed an increase of annexin V/PI positive cell population in a dose dependent fashion (06–40% at 10 and 20 μM respectively). This result suggested induced apoptosis with the compound (Figure 2). **31** treated Jurkat-E6.1 cells revealed a significant dose dependent increase in annexinV/PI positive population (17% at 2 μM, 53% at 5 μM) compared with untreated control (Figure 2).

Mitochondrial membrane potential assay

Mitochondrion are a major source of signals that initiate apoptotic cell death [37], and also a key regulator of caspases which have a major role in apoptosis. Mitochondrial dysfunction is associated with apoptosis induction. The transmembrane potential of the mitochondria was evaluated using JC 1, a lipophilic cationic dye, as a probe. **18** yielded a dose dependent drop in mitochondrial membrane potential (29% at a 10 μM and 65% at 20 μM dose) (Figure 3). A significant decrease in membrane potential was observed for **31** while treated in Jurkat-E6.1 cells at (47% at 2 μM and 75% at 5 μM dose) compared with the normal cells (Figure 3). This result also supported that both these compounds followed the induced apoptosis mechanisms in Jurkat-E6.1 leukemia cell line.

Table 2. Cytotoxicity of compounds against a variety of cancer cell lines.

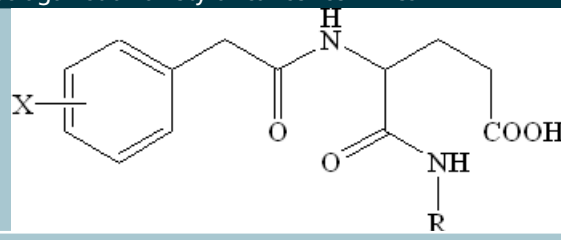

Compound	X	R	Cytotoxicity (μM)							
			U937	Jurkat-E6.1	MOLT-4	MDA-MB-231	MCF-7	HEPG-2	HUT-78	PBMC
1	H	*n*-But	49.88 ± 2.5	35.89 ± 1.1	33.87 ± 1.1	>200	24%	>400	>250	>400
2	H	*i*-But	97.86 ± 3.9	92.63 ± 2.6	93.20 ± 1.5	>200	>400	24%	>250	>400
3	H	*n*-Pent	35.82 ± 4.2	19.37 ± 3.3	23.54 ± 0.7	>200	>400	27%	>250	>400
4	H	*c*-Hex	31.57 ± 0.4	21.11 ± 0.7	41.89 ± 0.3	>200	34%	380	>250	>400
5	H	Ph	25.99 ± 1.5	16.54 ± 1.3	12.81 ± 2.4	>200	>400	>400	>250	>400
6	2-Me	Ph	69.33 ± 2.6	63.93 ± 0.6	52.57 ± 3.1	>200	>400	>400	>250	>400
7	2-F	*n*-Pr	69.92 ± 4.1	53.83 ± 0.7	61.39 ± 2.0	>200	ND	34%	>250	>400
8	2-F	*i*-Pr	73.58 ± 1.9	51.34 ± 2.1	52.39 ± 1.8	>200	26%	>400	>250	>400
9	2-F	*i*-But	39.57 ± 2.6	23.82 ± 4.2	19.85 ± 2.6	>200	280	23%	>250	>400
10	2-Cl	*n*-But	54.37 ± 1.2	26.54 ± 3.1	21.33 ± 0.9	>200	>400	>400	>250	>400
11	2-Cl	*n*-Hex	87.36 ± 0.7	81.29 ± 4.2	80.54 ± 1.1	>200	>400	>400	>250	>400
12	4-OMe	*t*-But	75.86 ± 3.1	50.21 ± 2.7	47.85 ± 0.7	>200	>400	21%	>250	>400
13	4-Br	*n*-Pr	49.98 ± 2.1	28.99 ± 2.9	29.15 ± 2.2	>200	ND	ND	>250	>400
14	4-Br	*n*-But	54.51 ± 4.2	29.82 ± 2.5	32.33 ± 0.9	>200	32%	>400	>250	>400
15	4-Br	*i*-But	62.73 ± 1.4	39.85 ± 2.0	38.51 ± 1.5	>200	310	370	>250	>400
16	4-Br	*c*-Hex	49.35 ± 3.1	13.51 ± 3.3	15.61 ± 1.4	>200	22%	24%	>250	>400
17	4-Cl	*n*-Pr	76.8 ± 2.6	17.25 ± 0.6	37.85 ± 4.1	>200	12%	>400	>250	>400
18	4-Cl	*i*-Pr	29.36 ± 0.5	11.50 ± 0.5	11.80 ± 2.6	>200	250	15%	>250	>400
19†	H	*n*-Pr	55.47 ± 0.8	5.14 ± 5.2	8.23 ± 1.8	>200	40%	42%	>250	>400
20†	H	*i*-Pr	59.61 ± 2.3	18.76 ± 0.3	23.63 ± 1.1	>200	18%	>400	>250	>400
21†	H	*t*-But	31.54 ± 5.1	27.63 ± 0.2	23.69 ± 2.0	>200	44%	>400	>250	>400
22†	H	Bnz	66.59 ± 2.3	63.74 ± 1.7	61.77 ± 1.4	>200	36%	370	>250	>400
23†	4-OMe	Bnz	44.21 ± 3.3	25.32 ± 0.6	26.89 ± 3.5	>200	42%	35%	>250	>400
24†	4-OMe	*i*-But	85.92 ± 1.4	43.24 ± 4.3	41.98 ± 2.3	>200	>400	27%	>250	>400
25†	2-Cl	Bnz	42.93 ± 2.5	32.95 ± 4.2	33.97 ± 1.8	>200	>400	37%	>250	>400
26†	2-Cl	*i*-But	54.32 ± 0.7	27.84 ± 3.6	25.19 ± 2.9	>200	350	>400	>250	>400
27†	2-Cl	*n*-Pent	66.94 ± 3.6	34.23 ± 2.9	37.81 ± 2.4	>200	>400	>400	>250	>400
28†	4-Br	Bnz	37.85 ± 1.1	11.16 ± 2.6	9.32 ± 2.6	>200	290	270	>250	>400
29†	4-Br	*n*-Hex	43.98 ± 4.3	19.56 ± 4.1	21.33 ± 1.8	>200	290	320	>250	>400
30†	4-Br	*n*-Pent	71.24 ± 3.9	8.97 ± 4.2	11.35 ± 0.8	>200	>400	>400	>250	>400
31†	4-Br	4-NO_2Bnz	10.59 ± 2.8	2.77 ± 0.6	4.58 ± 0.3	>200	37%	24%	>250	>400
32†	4-Cl	*n*-Hex	23.62 ± 2.5	12.57 ± 0.7	11.91 ± 1.1	>200	280	250	>250	>400
33†	2,4-diCl	*n*-Hex	32.94 ± 0.7	11.37 ± 0.8	21.93 ± 1.3	>200	220	280	>250	>400
34†	2,4-diCl	Bnz	39.44 ± 2.1	23.86 ± 0.9	25.32 ± 0.6	>200	210	220	>250	>400
35†	$(=CH)_4$	*n*-Hex	44.32 ± 1.2	30.95 ± 3.1	28.33 ± 2.4	>200	270	240	>250	>400

†From Ref. [3].
ND: Not determined; PBMC: Peripheral blood mononuclear cell.

Table 3. Selectivity study (IC_{50} PBMC/IC_{50} cell line).

Compound	Selectivity index		
	Jurkat E6.1	U937	Molt-4
1	11.14 ± 0.67	8.01 ± 2.1	11.80 ± 2.7
2	4.32 ± 1.7	4.08 ± 1.9	4.29 ± 0.9
3	20.7 ± 2.2	11.16 ± 2.7	16.99 ± 1.8
4	18.9 ± 3.4	12.67 ± 3.1	9.54 ± 2.2
5	24.18 ± 4.2	15.39 ± 0.7	31.22 ± 1.8
6	6.25 ± 3.5	5.76 ± 1.3	7.60 ± 3.0
7	7.43 ± 2.1	5.72 ± 0.9	6.51 ± 0.7
8	7.79 ± 0.7	5.43 ± 0.6	7.63 ± 0.9
9	16.79 ± 1.6	10.10 ± 1.5	20.15 ± 2.0
10	15.07 ± 2.5	7.35 ± 1.4	18.75 ± 1.4
11	4.92 ± 1.1	4.57 ± 4.2	4.96 ± 2.5
12	7.96 ± 0.8	5.27 ± 3.1	8.35 ± 3.4
13	13.79 ± 1.5	8.00 ± 3.6	13.72 ± 2.7
14	13.41 ± 2.31	7.33 ± 4.2	12.37 ± 2.0
15	10.03 ± 3.1	6.37 ± 2.4	10.38 ± 1.5
16	28.96 ± 1.4	8.10 ± 2.6	25.62 ± 1.1
17	23.18 ± 0.5	5.20 ± 2.5	10.56 ± 0.9
18	34.78 ± 0.7	13.62 ± 2.7	33.89 ± 0.3
19	6.27 ± 3.4	7.21 ± 1.5	48.60 ± 0.5
20	15.97 ± 1.0	6.71 ± 0.6	16.92 ± 0.7
21	9.25 ± 0.8	12.62 ± 1.1	16.88 ± 1.2
22	77.82 ± 1.3	6.00 ± 1.9	6.47 ± 1.7
23	21.32 ± 0.3	9.04 ± 2.5	14.87 ± 1.4
24	14.47 ± 2.0	4.65 ± 0.7	9.52 ± 2.7
25	12.13 ± 2.1	9.31 ± 2.1	11.77 ± 3.7
26	14.36 ± 4.1	7.36 ± 2.5	15.87 ± 3.3
27	11.68 ± 3.3	5.97 ± 0.8	10.57 ± 3.7
28	35.86 ± 2.7	10.56 ± 2.3	42.91 ± 4.3
29	20.44 ± 1.5	9.09 ± 1.0	18.75 ± 2.8
30	44.59 ± 0.4	5.61 ± 0.5	35.24 ± 2.7
31	144.40 ± 2.0	37.77 ± 1.5	87.33 ± 3.9
32	31.82 ± 1.6	16.93 ± 1.1	33.58 ± 2.5
33	35.18 ± 2.5	12.14 ± 2.3	18.23 ± 2.2
34	16.76 ± 1.7	10.14 ± 2.5	15.79 ± 3.1
35	12.92 ± 1.5	9.02 ± 1.4	14.11 ± 1.7

Flow cytometry analysis of MMP 2 & HDAC8 expressions

The changes in MMP-2 and HDAC8 expression levels in Jurkat-E6.1 cells before and after treatments with **18** and **31** were estimated by flow cytometry analysis [3,36,38]. The treated and untreated cells were fixed and stained with either MMP-2 or HDAC8 antibody followed by treatment with secondary antibody conjugated with FITC. The Jurkat-E6.1 cell population with MMP 2 and HDAC8 cells were found to be reduced significantly after treatment with **18** and **31** in a dose dependent manner (Figure 4A & B).

Compound **31** treated Jurkat-E6.1 cells showed a reduction of 46% (2 μM) and 70% (5 μM) in MMP-2 expression compared with untreated cells. The reduction was 48% (2 μM) and 68% (5 μM) for HDAC8 expression. On the other hand, compound **18** treatment on Jurkat-E6.1 cells showed 42 % (10 μM) and 58% (20 μM) reduced MMP-2 expression than the untreated cells and for HDAC8 the decrease of expression was 32% (10 μM) and 58% (20 μM).

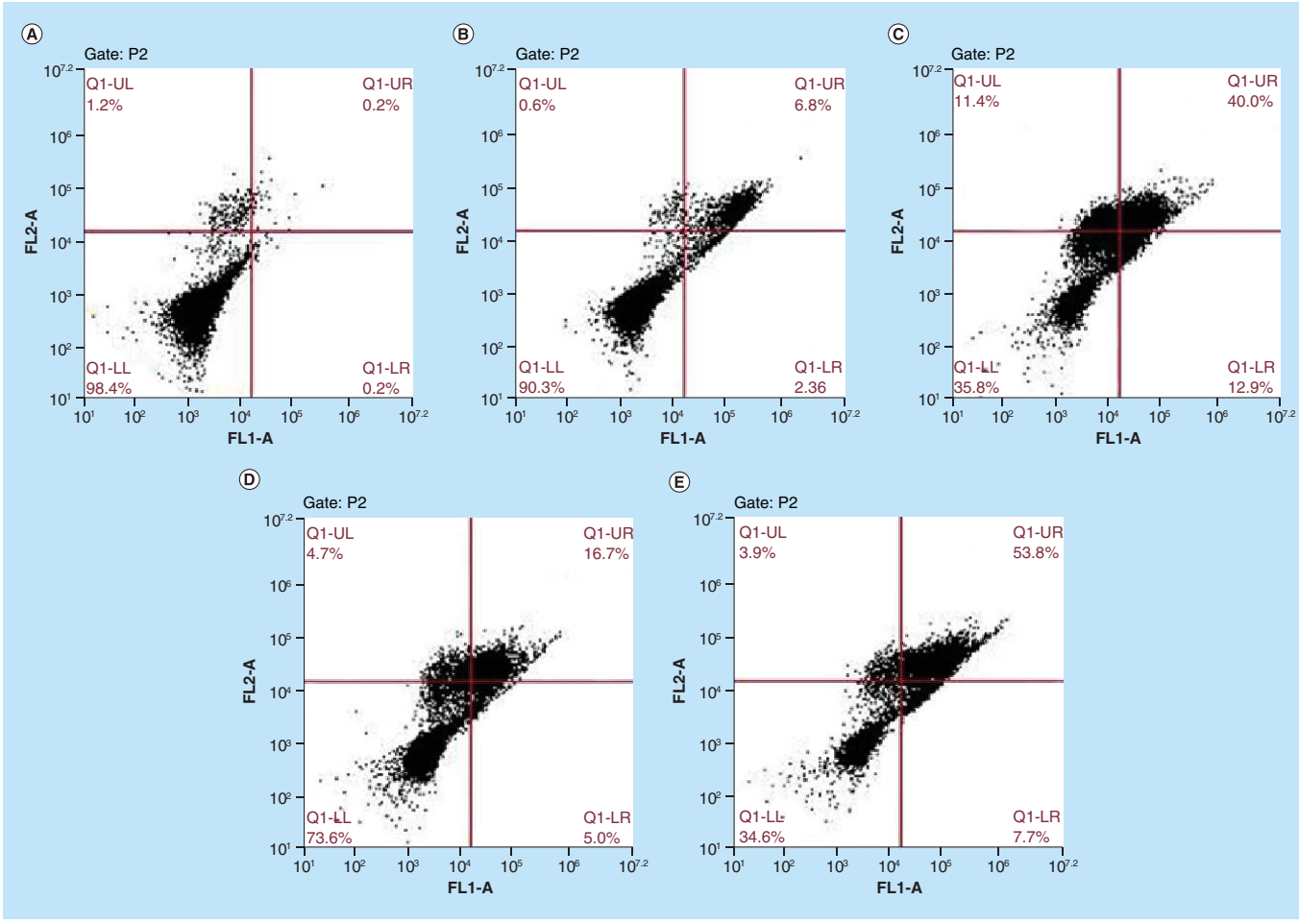

Figure 2. AnnexinV-FITC/PI assay, flow cytometric analysis in Jurkat-E6. 1 cells **(A)** untreated, **(B)** treated with **18** (10 μM), **(C)** treated with**18** (20 μM), **(D)** treated with **31** (2 μM), **(E)** treated with **31** (5 μM).

DNA nick generation assay

In order to determine if there is any nicked DNA, the 4',6-diamidino-2-phenylindole (DAPI) stain was used as it produces fluorescence while binding to the nicked DNA [3,36,38]. DAPI is a DNA specific probe that forms a fluorescent complex by attaching to the A-T rich region of DNA. If there is any nicked DNA, DAPI will produce an increase in the fluorescence as DAPI binds into the nicked portion of the DNA [28]. As **31** was the best cytotoxic compound against Jurkat-E6.1 cell line (IC_{50} = 2.77 μM), it was subjected to further screen for DNA nick generation study in Jurkat-E6.1 cell line. After DAPI staining, the untreated or **31**-treated cells were visualized under fluorescence microscope. It was interesting to note that there was no fluorescence for the untreated Jurkat-E6.1 cells (Figure 4C–E) whereas an increase in the intensity of DAPI fluorescence was noticed in the **31**-treated Jurkat-E6.1 cells after 48 h. of incubation (Figure 4C–E). It was noticed that **31** produced better nicks in the DNA of Jurkat-E6.1 cells at higher doses compared with the lower dose (Figure 4C–E). The fluorescence was found to be higher in Jurkat-E6.1 cells in a dose-dependent manner (Figure 4C–E). This dose-dependent increase in the fluorescence of DAPI suggested that **31** was effective in producing the nick in the DNA and reflected the ability to induce apoptosis in Jurkat-E6.1 cells.

Cell cycle assay

The cell cycle assay is performed usually by flow cytometry after staining cells with propidium iodide (PI) followed by treatment with RNAse [36]. As far as the cell cycle analysis is concerned, it determines the stage of the cell cycle where the cell population is arrested. An increased number of cell populations in the sub-G0 stage indicate cellular apoptosis. In this study, a prominent increase of 18% in the sub diploid (sub-G0) cell population was noticed after

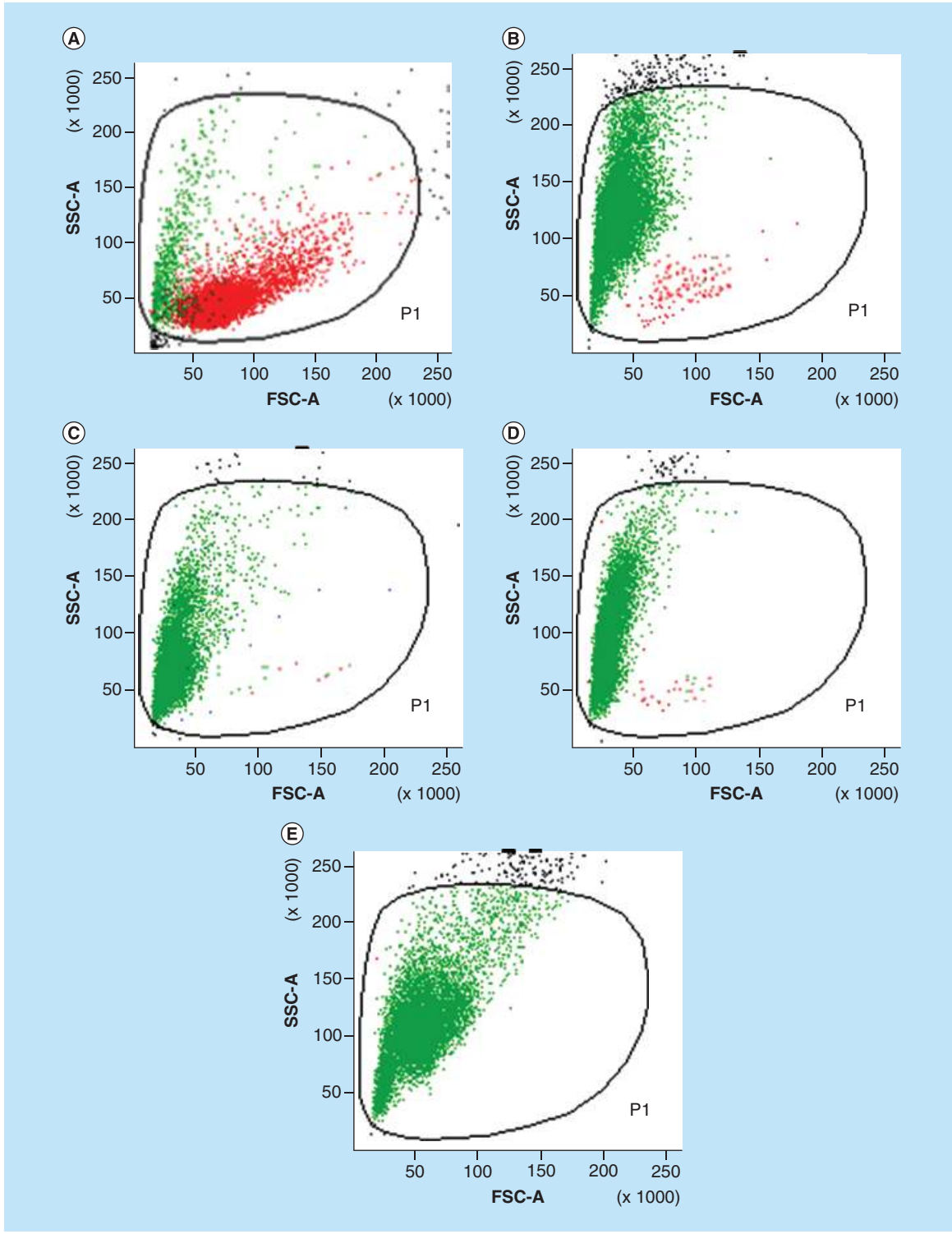

Figure 3. AnnexinV-FITC/PI assay, flow cytometric analysis in Jurkat-E6.1 cells by flow cytometric assay with JC1 dye in five groups. (A) control/ untreated, **(B)** treated with **18** (10 μM), **(C)** treated with **18** (20 μM), **(D)** treated with **31** (2 μM), **(E)** treated with **31**(5 μM).

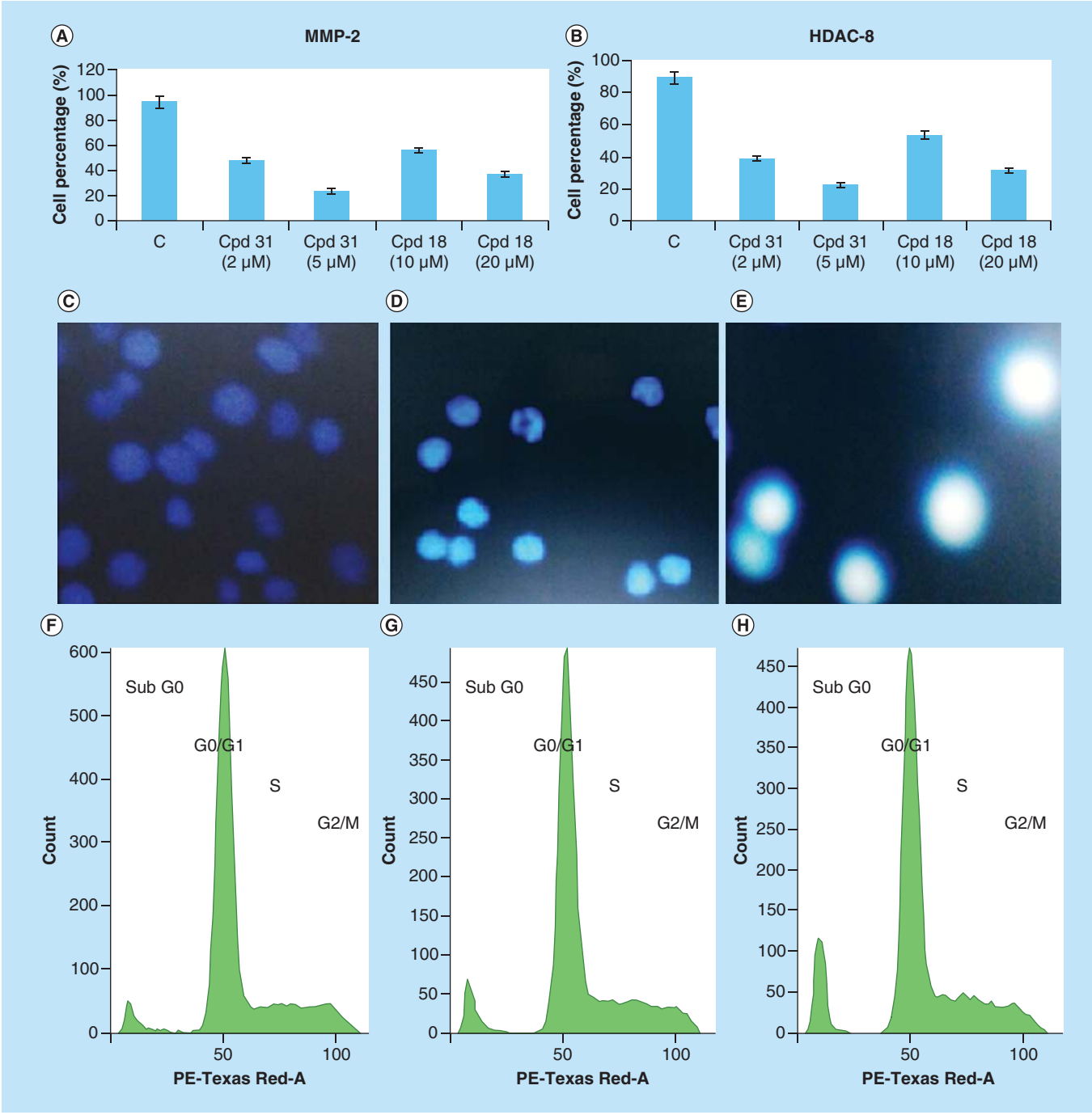

Figure 4. AnnexinV-FITC/PI assay, flow cytometric analysis in Jurkat-E6. A comparative **(A)** MMP-2 and **(B)** HDAC8expression analysis of control or untreated and **31** and **18** treated Jurkat-E6.1 cells by flow cytometry. **(C–E)** Fluorescence imaging for DNA nick generation assay with Jurkat-E6.1cells; **(C)** untreated, **(D)** treated with **31** (2 μM), **(E)** treated with **31** (5 μM). **(F–H)** Cell cycle analysis of Jurkat-E6.1 cells after PI staining; **(F)** Untreated control, **(G) 31** treated at 2 μM ,**(H) 31** treated at 5 μM showing the arrest of cell cycle in sub-G0 stage.

treatment with **31** in Jurkat-E6.1 cell at a dose of 2 μM (Figure 4F–H). Moreover, a dose dependent increase in the G1 population from 18 to 27% indicated that **31** is a potential molecule that blocks the cell cycle progression and moves the cell toward apoptosis (Figure 4F–H).

10.4155/fmc-2018-0361

SAR study

All these newly synthesized compounds (**1–18**) of Table 2 displayed moderate cytotoxicity in U937, Jurkat-E6.1 and Molt-4 leukemia cell lines. Regarding cytotoxicity against U937, it was noticed for the unsubstituted phenylacetyl analogs that aryl substitution such as the phenyl ring at R position (**5**) resulted in better efficacy than the linear (**1**, **3**) or branched alkyl (**2**) as well as the cyclic aliphatic (**4**) substitution. Again, *c*-hexyl (**4**) substitution was found to be better than the *n*-pentyl (**3**) or *n*-butyl (**1**) and the linear alkyl substitutions were better than the branched alkyl substitution such as *i*-butyl (**2**) at R position (Table 2). However, more than 2.5-fold reduction in cytotoxicity was noticed for compound with methyl substitution at the *ortho* position of the phenyl ring (**6** vs **5**). For the fluoro substituted analogs (X = F), the *i*-butyl substitution (**9**) at R position resulted in 2-fold better inhibition compared with the *i*-propyl (**8**) or n-propyl (**7**) substitution. Comparing the activity of compounds **7–11**, it was observed that the branched alkyl substitution at R position is better than the linear alkyl substitution (**9** vs **10**, **11**; Table 2). It was interesting to note that *p*-bromo substitution (X = 4-Br) at the phenylacetyl moiety was better than the *o*-chloro (X = 2-Cl) or *o*-fluoro (X = 2-F) substitution. However, comparing **17** and **18**, it may be noticed that **18** was more than 2.5-fold better cytotoxic than **17**. Therefore, it may be assumed that *i*-propyl (**18**) substitution at R position is better than *n*-propyl (**17**) substitution. As far as the MOLT-4 cytotoxicity was concerned, all these compounds displayed similar type of cytotoxicity compared with the Jurkat-E6.1 cellular toxicity (Table 2).

It was interesting to note that compared with U937, these newly synthesized compounds (**1–18**) exhibited better cytotoxicity in Jurkat-E6.1 cell line. Regarding cytotoxicity in Jurkat-E6.1 cell line, it was noticed that the methyl substitution at the *ortho* position of the phenylacetyl function (X = 2-CH_3) reduced fourfold cellular toxicity (**6** vs **5**). It was also interesting to note that for the unsubstituted analogs (X = H), increasing the linear chain length at R position enhanced Jurkat-E6.1 cell cytotoxicity (**3** vs **1**; Table 2). However, branching at the alkyl chain reduced the cytotoxicity (**2** vs **1** and **3**). Again, cyclic aliphatic group such as *c*-hexyl (**4**) and aryl group such as phenyl (**5**) at R position yielded potential Jurkat-E6.1 cell cytotoxicity. Again, *o*-fluoro (**7**, **8**) and *o*-chloro (**11**) as well as *p*-methoxy (**12**) substituted compounds (X = 2-Cl, 2-F, 4-OCH_3) were lesser cytotoxic in Jurkat-E6.1 cell line. However, *p*-bromo (**13–16**) or *p*-chloro (**17–18**) phenylacetyl compounds (X = 4-Br, 4-Cl) were comparatively better cytotoxic than the unsubstituted compounds (**1–5**) or *o*-chloro (**10–11**) or *o*-fluoro (**7–9**) compounds (X = 2-Cl, 2-F; Table 2). Therefore, it may be assumed that bulky electron withdrawing substitutions such as bromo or chloro at the *para* position of the phenylacetyl moiety (X = 4-Br, 4-Cl) is better favorable than the unsubstituted analogs (**14**> **1**; **15**> **2**; **16**> **4**). However, cyclic aliphatic substitution such as *c*-hexyl (**16**) at R position resulted in better Jurkat-E6.1 cell cytotoxicity compared with linear (such as *n*-propyl [**13**], *n*-butyl [**14**]) or branched alkyl (such as *i*-butyl [**15**]) substitution at the same position. However, *p*-chlorophenyl substitution (X = 4-Cl) with *n*-propyl group at R position was found better than the corresponding *p*-bromophenyl compound (X = 4-Br; **17** > **13**). Again, *i*-propyl substitution is better than the *n*-propyl substitution (**18** > **17**; Table 2).

All these compounds were inactive in MDA-MB-231 and MCF-7 breast cancer cell lines. However, **9**, **15** and **18** exhibited lower efficacy in MCF-7 cell line with an IC_{50} values of 280, 310 and 250 μM, respectively. These three compounds either possess branched alkyl substitution such as *i*-butyl (**9**, **15**) or *i*-propyl (**18**; Table 2). Therefore, it may be assumed that branched alkyl substitution is required for imparting cytotoxicity in MCF-7 cell line compared with the linear or cyclic aliphatic substitution. Again, *i*-propyl substitution (**18**) is better than the *i*-butyl (**9**, **15**) substitution. Except for **4** and **15**, all these compounds were found inactive against HEPG-2 cell line (Table 2). Moreover, all these compounds were inactive in HUT cell line. It was interesting to note that these compounds were inactive against peripheral blood mononuclear cell (PBMC) line. Combining all the cytotoxicity results of newly synthesized compounds, it may be assumed that *p*-chloro or *p*-bromophenylacetyl compounds (X = 4-Cl or 4-Br) were better cytotoxic than the unsubstituted compounds. Nevertheless, branched alkyl or cyclic aliphatic or aryl moiety at R position was better than the linear alkyl substitution. One most important observation noticed from the cytotoxicity was that these compounds exhibited cytotoxicity only against leukemia cell lines (U937, Jurkat-E6.1, Molt-4) but inactive in solid tumor cell lines (MDA-MB-231, MCF-7, HEPG-2).

Similar to the compounds of current study (**1–18**), earlier reported **19–35** [3] were found to be cytotoxic against U937 (IC_{50} <90 μM), Jurkat-E6.1 (IC_{50} <70 μM) and Molt-4 (IC_{50} <70 μM) cell lines. These compounds showed inactivity against MDA-MB-231 (IC_{50} >200 μM), Hut-78 (IC_{50} >250 μM) and PBMC (IC_{50} >400 μM). However, some of these compounds were moderately active against MCF-7 and HEPG-2 cell lines (Table 2).

Regarding the cytotoxicity against U937 cell lines, it was observed that the benzyl substitution at R position (**23**, **25**, **28**, **34**) resulted in effective cytotoxicity. Again, strong electron-withdrawing substituent at the *para* position of

the benzyl moiety at R position resulted in more than threefold U937 cytotoxicity (**31** vs **28**; Table 2). Interestingly, long chain linear alkyl substitution such as *n*-hexyl at the R position also yielded potent cytotoxicity (**29**, **32**, **33**, **35**) compared with the smaller linear alkyl such as *n*-propyl (**19**) or branched chain alkyl substitution such as *i*-propyl (**20**) and *i*-butyl (**24**, **26**) at the same position (Table 2). However, more branching at the R position such as *t*-butyl (**21**) yielded potent U937 cytotoxicity. It was also interesting to note that *n*-pentyl substitution at R position (**27**, **30**) resulted in poor cytotoxicity. Again, 2,4-dichloro substitution (**33**, **34**) at X position was better favorable than the 2-chloro (**25**–**27**), 4-methoxy (**23**–**24**) or 4-bromo (**28**–**30**) substitutions at the same position. Naphthyl group (**35**) also produced effective U937 cytotoxicity (Table 2). Therefore, it may be postulated that six methylene units or higher branching at the alkyl moiety at R position as well as bulky aryl groups or bulky electron-withdrawing functions at the aryl moiety should be required for imparting higher U937 cytotoxicity.

A similar phenomenon was observed for these compounds for their cytotoxicity against Jurkat-E6.1 and Molt-4 cell lines. However, these compounds were better cytotoxic against both these Jurkat-E6.1 and Molt-4 cell lines compared with U937. For both these cell lines, benzyl (**25**, **28**, **34**) or higher linear alkyl such as *n*-pentyl (**27**, **30**) and *n*-hexyl (**29**, **32**, **33**, **35**) as well as branched alkyl substitution such as *i*-butyl (**24**, **26**) and *t*-butyl (**21**) substitution at R position yielded potential cytotoxicity. However, *p*-nitrobenzyl substitution resulted in the maximum cytototoxicity against these cell lines (Table 2).

Therefore, combining the cytotoxicities of compounds of current study (**1–18**) and the earlier reported compounds [3], it may be postulated that higher linear alkyl function (more than *n*-pentyl) or higher branched alkyl (such as *i*-butyl or *t*-butyl) as well as bulkyl aryl (such as benzyl) or electron-withdrawing bulky aryl group (such as *p*-nitrobenzyl) at R position should be important factors for imparting higher cellular toxicity.

Binding mode interaction studies

Due to the promising cytotoxicity, **18** (the highest active newly synthesized compound) was docked into the active sites of four zinc-dependent metalloenzymes (namely MMP-2, MMP-9, HDAC8 and APN) by Maestro software of Schrodinger Inc. (MA, USA) [39,40] to know the probable enzyme-ligand binding interactions. Molecular docking studies of **31** (the highest active earlier reported compound) with MMP-2 and HDAC8 were already reported earlier [3]. Nevertheless, **31** was also docked into the active site of MMP-9 and APN. Both of these compounds perfectly docked into the active site of all these metalloenzymes. Figure 5A & B depicts the docking interactions of **18** with the MMP-2 (PDB: 1HOV) active site.

As the carboxylic acid moiety is a metal chelating group, **18** was found to form a salt bridge interaction with catalytic Zn^{2+} ion of MMP-2 (PDB: 1HOV). It was noticed that the carbonyl oxygen atom associated with the *i*-propylamido moiety accepts hydrogen bonds from the amino acid residues Leu83 and Ala84. The flexibility of aminoacetyl moiety associated with the chiral carbon atom directed the *p*-chlorophenyl group towards the S2′ pocket instead of hydrophobic S1′ pocket. However, the *i*-propyl group was lying closely at the S1′ pocket formed by the amino acid residues namely His120, Tyr142, Ala139, Ile141, val117 and His85. The docking interactions of the 4-chlorophenylacetyl analog (X = 4-Cl) were in close agreement with the earlier docking observations [3,38,40]. Apart from strong chelation with the catalytic Zn^{2+} ion by carboxylic acid moiety, **31** also exhibited a hydrogen bonding interaction with Leu83 through the carbonyl group adjacent to the *p*-nitrobenzylamino moiety. Moreover, the amido group adjacent to the *p*-bromophenylactyl moiety formed another hydrogen bonding interaction with Gly81 [3].

Regarding the HDAC8-**18** binding interactions, it was observed (Figure 5C & D) that the phenyl group formed a π–π stacking interaction with the hydrophobic amino acid residue Trp141 at the HDAC8 enzyme active site (PDB: 1VKG). The hydroxyl group of the carboxylic acid moiety chelates strongly to the catalytic Zn^{2+} ion (Figure 5C & D). The catalytic Zn^{2+} ion formed an additional salt-bridge interaction with the carbonyl group adjacent to the *i*-propylamido moiety. The carbonyl function of the carboxylic acid group accepts a hydrogen bond from the polar amino acid residue His142 at the enzyme active site. The ligand docking interaction with HDAC8 enzyme was in close agreement with the earlier observation [3]. The docking interaction between the HDAC8 and **31** suggested that the phenyl ring of **31** formed a π–π stacking interaction with Trp141 [3].

Both **18** and **31** were also docked into the active site of MMP-9 enzyme (PDB: 2OW1; Figure 6).

The docking study revealed that the carboxylic acid group of **18** had a salt bridge interaction with the catalytic Zn^{2+} ion (Figure 6). Interestingly, it was observed that the *p*-chlorophenyl moiety inserted towards the S1′ pocket lined by the amino acid residues Tyr420, Ala417, Arg424, Tyr423, Leu397, Leu418, His401 and Val398. The phenyl group was also found to form a π–π stacking interaction with Tyr423. Nevertheless, the amido group

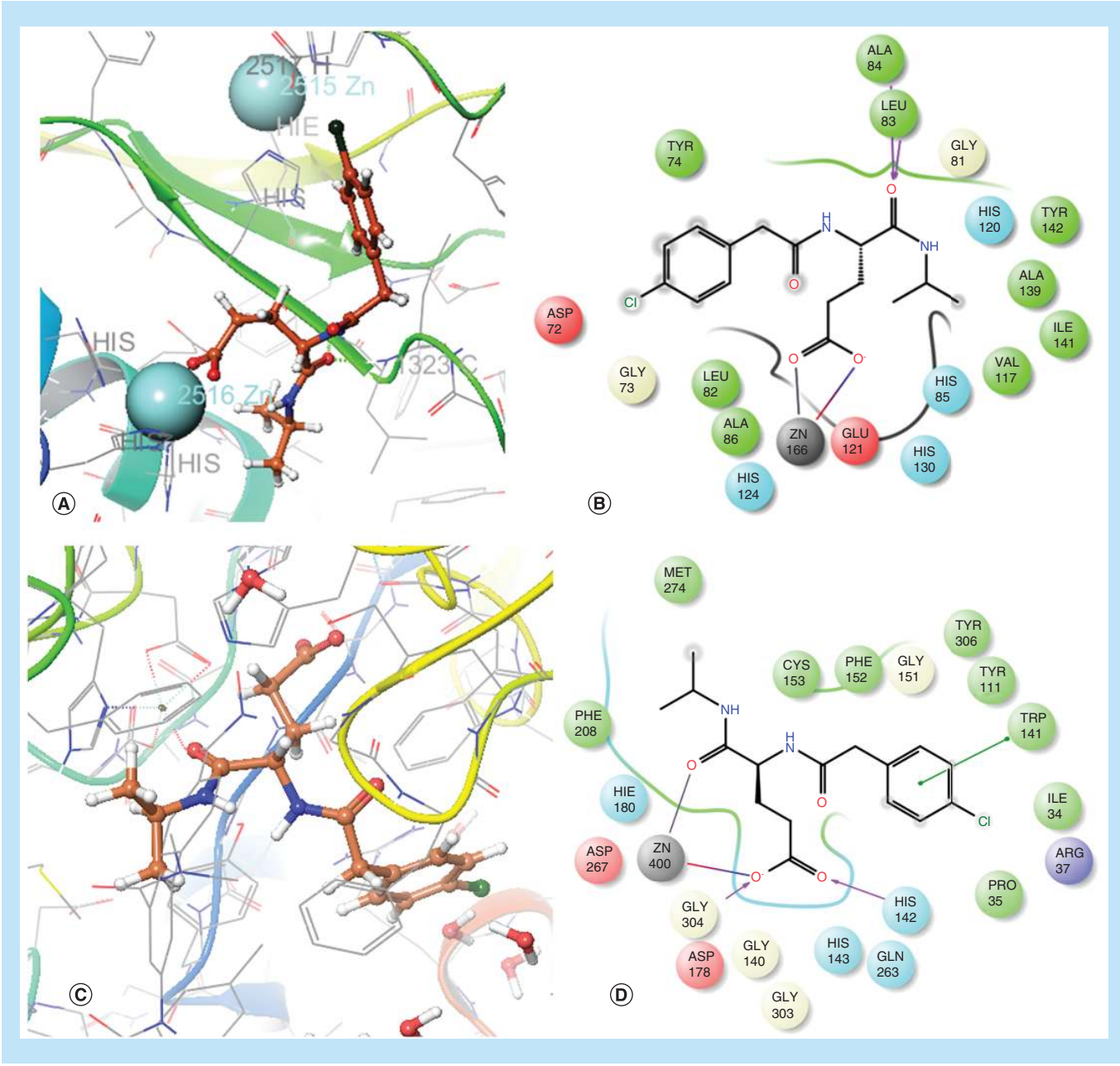

Figure 5. AnnexinV-FITC/PI assay, flow cytometric analysis in Jurkat-E6. (A) 3D and **(B)** 2D interaction plots the best active **18** with MMP-2 enzyme (PDB: 1HOV). Zn^{2+} is shown as cyan ball in the 3D interaction plot. **(C)** 3D and **(D)** 2D interaction plots the best active **18** with HDAC8 enzyme (PDB: 1VKG). Zn^{2+} is shown as green small ball in the 3D interaction plot.

of the isopropylamide moiety was found to act as a hydrogen bond donor with Pro421 whereas the adjacent carbonyl oxygen atom acted as a hydrogen bond acceptor with Leu188. The docking interaction of **31** also showed a π–π stacking interaction with Tyr423 with the *p*-nitrophenyl moiety. The carbonyl function associated with the *p*-bromophenylacetyl moiety of **31** also had a hydrogen bonding interaction with Tyr423. Moreover, the amido function adjacent to the carbonyl group also formed a hydrogen bond interaction with Gly186 (Figure 6).

These compounds (**18** and **31**) were further docked into the APN enzyme active site (PDB: 4FYR). The carboxylic group was found to chelate with the Zn^{2+} ion in a bidentate fashion to form a four membered-ring system (Figure 7).

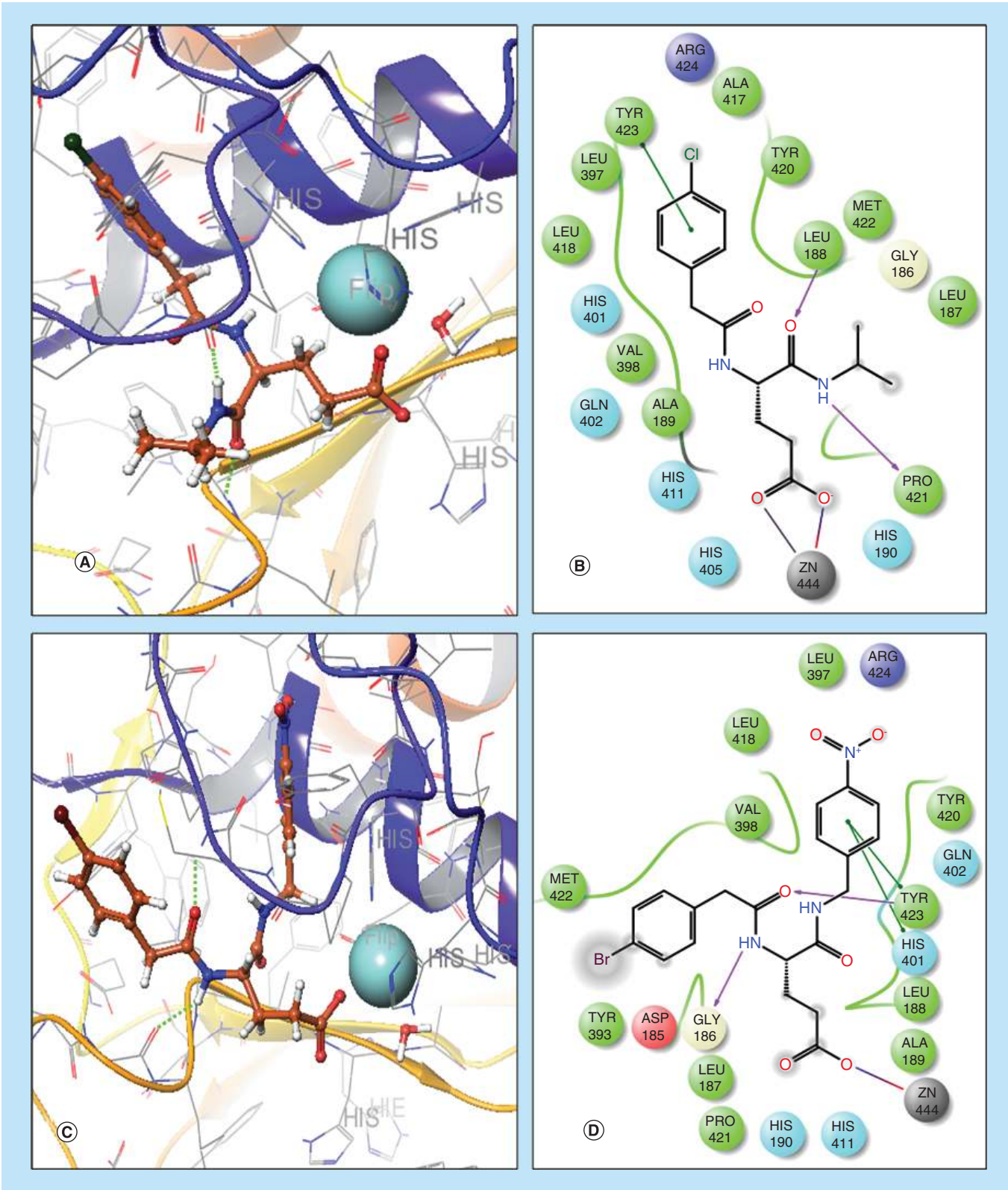

Figure 6. AnnexinV-FITC/PI assay, flow cytometric analysis in Jurkat-E6. (A) 3D and **(B)** 2D interaction plots of **18** with MMP-9 enzyme. **(C)** 3D and **(D)** 2D interaction plots of **31** with MMP-9 enzyme (PDB: 2OW1). Zn^{2+} is shown as cyan ball in the 3D interaction plot.

10.4155/fmc-2018-0361

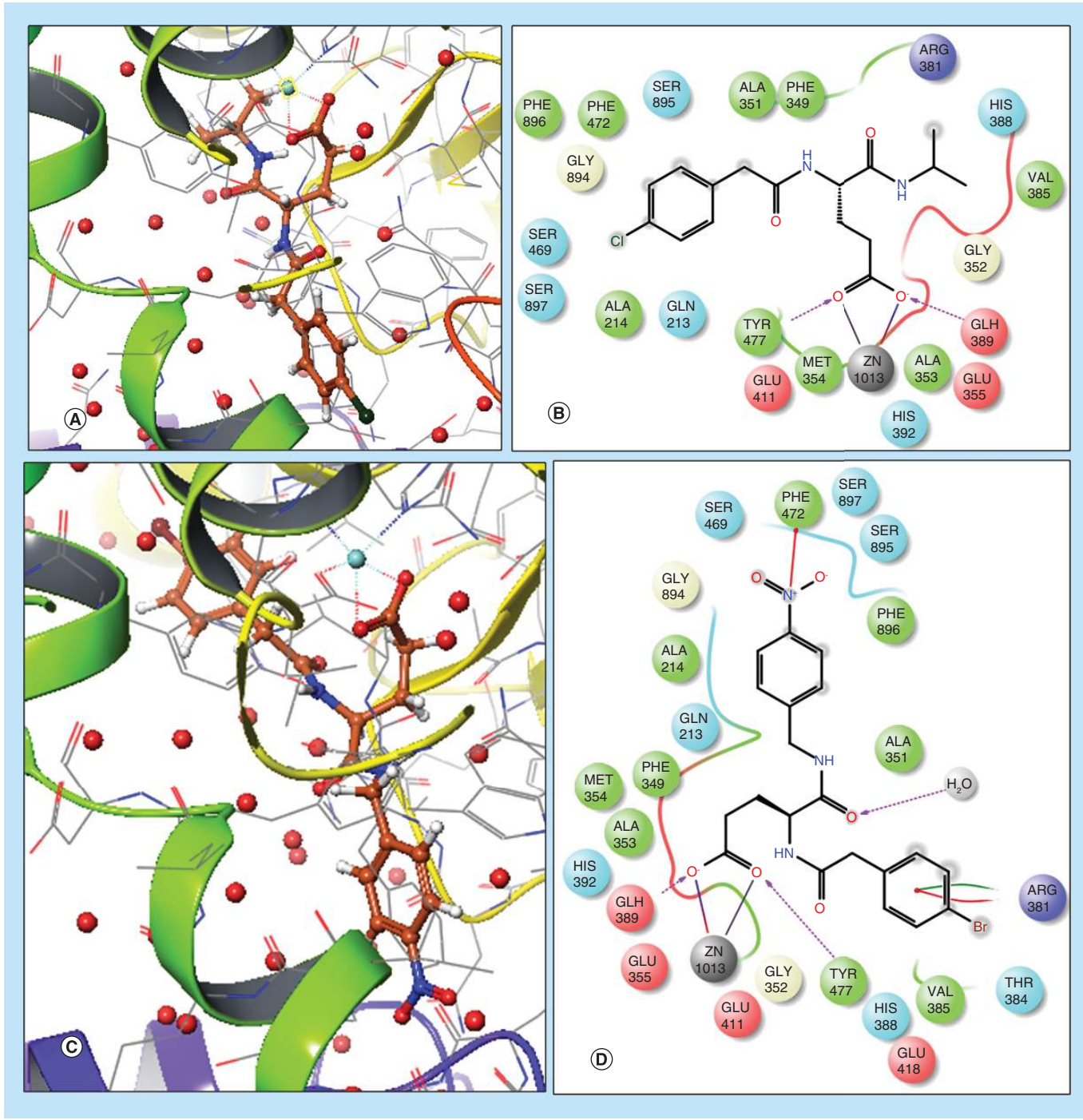

Figure 7. AnnexinV-FITC/PI assay, flow cytometric analysis in Jurkat-E6. (A) 3D and **(B)** 2D interaction plots of **18** with APN enzyme; **(C)** 3D and **(D)** 2D interaction plots of **31** with APN enzyme (PDB: 4FYR). Zn^{2+} is shown as cyan small ball in the 3D interaction plot.

Moreover, the hydroxyl and carbonyl functions of both of these compounds were found to accept hydrogen bonds from amino acids Gln389 and Tyr477, respectively. Again, an additional hydrogen bonding interaction was noticed between the carbonyl group and an essential water molecule at the enzyme active site for **31**. The nitro group of **31** was found to interact with Phe 472.

Therefore, it may be inferred from binding interactions between these metalloenzymes (MMP-2, MMP-9, HDAC8 and APN) with **18,** as well as **31,** that these compounds may exert the anticancer effects through blocking

their enzymatic effect via down regulating pathways associated with these metalloenzymes. Moreover, it may be validated that such type of derivatives may simultaneously block the action of these metalloenzymes to impart their potential antileukemic efficacy.

Conclusion

From this current study, it is confirmed that none of these compounds are active against solid tumors (such as MDA-MB-231, MCF-7 and HEPG-2). However, some of them exhibited better efficacy against leukemia cells, specifically T-acute lymphocytic leukemia (Jurkat-E6.1 and MOLT-4). A number of compounds (**3**, **5**, **16–20** and **28**–**33**) showed better cytotoxic efficacy (IC_{50} <20 μM) against Jurkat-E6.1 cell line. Again, some of them (**5**, **9**, **16**,**18, 19, 28** and **30**–**32**) also exhibited higher cytotoxic potential (IC_{50} <20 μM) against MOLT-4 cell line. **31** exhibited best cytotoxicity against all these leukemia cell lines (IC_{50} in U937 = 10.59 μM; IC_{50} in Jurkat-E6.1 = 2.77 μM and IC_{50} in MOLT-4 = 4.58 μM). It was interesting to note that except **31**, all these compounds were found to be moderately effective in U937 cell line. Interestingly, all these compounds were inactive in normal cell line PBMC. As these compounds had efficacy against leukemia cell lines and inactive against solid tumors as well as normal cell, it may be inferred that these compounds may only be targeted to treat leukemia. The best active compound (**31**), having structural similarity with these newly synthesized compounds (**1–18**) reported here, was a potential dual MMP-2 and HDAC8 inhibitor reported earlier [3]. The most effective compound (**18**) among these newly synthesized compounds (**1–18**) of the present series (Table 2) exhibited similar type of ligand-binding interactions with both MMP-2 and HDAC8 compared with **31** as evidenced by the molecular docking observations. Therefore, it may be inferred that these newly synthesized compounds (**1–18**) of this series may act through binding with both MMP-2 and HDAC8. Nevertheless, the docking interactions also suggested that these compounds may also bind to MMP-9 and APN which are validated targets of cancer. Therefore, these pentanoic acid derivatives reported here may act as tetrad metalloenzyme inhibitors targeted to the treatment of cancer. Moreover, **18** and **31** were also found to induce apoptosis effectively (38% at 20 μM and 53% at 5 μM, respectively) in a dose-dependent fashion as suggested by annexin V/PI apoptosis assay in Jurkat-E6.1 cell line. Both of these compounds also reduced the expression of both MMP-2 and HDAC8 effectively. **31** reduced 70% MMP-2 expression and 68% HDAC8 expression as seen in flow cytometry analysis. **31** also produced prominent intensity of fluorescence to bring nick in Jurkat-E6.1 cells suggesting the potentiality to induce apoptosis. **31** also showed cellular arrest in sub-G0 phase as evidenced by cell cycle analysis. The mitochondrial membrane potential assay also suggested that both these compounds exhibited induced apoptotic mechanisms in Jurkat-E6.1 leukemia cells. It is interesting to note that **31** showed unique properties of anti-migratory and anti-invasive effects in NSCLC cell line A549 reported earlier [3] and antileukemic effect in acute lymphoblastic leukemia cell line Jurkat-E6.1.

Future perspective

It may be postulated that such type of pentanoic acid derivatives may execute their antileukemic activity through simultaneous blocking of these zinc-dependent metalloenzymes. Therefore, this study may unveil a new vista to design newer pentanoic acid derivatives targeted to leukemia via blocking the activity of zinc-dependent metalloenzymes and may act as adjuvent chemotherapeutic agent in NSCLC.

Summary points

Substituted pentanoic acids as anticancer agents

- Substituted pentanoic acids may show promising effect against hemalotogical malignancy.
- These compounds show cytotoxicity against human leukemic cell lines namely Jurkat-E 6.1, U937 and MOLT-4.
- One of these compounds (**31**) showed good antileukemic effects in leukemia as well as can block migration and invasion in non-small-cell lung cancer reported earlier.
- One compound of this series (**31**) induces apoptosis and also exhibits cellular arrest in sub-G0 phase as evidenced by cell cycle analysis with Jurkat-E6.1 cell line.

Metalloenzyme inhibitors as an emerging agent against cancer

- Molecular docking interaction study supported that these derivatives may effectively bind to metalloenzymes (MMP-2, MMP-9, HDAC8 and APN) to exert their enzyme inhibitory potential.
- This study may provide an aspect of designing newer pentanoic acid derivatives with anticancer profile in future.

10.4155/fmc-2018-0361

Financial & competing interest disclosure

S Dutta is thankful to University Grant Commission, New Delhi, India for providing DS Kothari Postdoctoral Fellowship. N Adhikari is thankful to University Grant Commission, New Delhi, India for providing Rajiv Gandhi National Fellowship. SA Amin sincerely acknowledge Jadavpur University, Kolkata for awarding Junior Research Fellowship to work in the Department of Pharmaceutical Technology under State Government Fellowship Scheme of Jadavpur University, Kolkata, India. T Jha is thankful to the Universities with Potential for Excellence program, Phase II of Jadavpur University sanctioned by University Grants Commission, New Delhi, India for funding. Authors are also thankful to the authority of Jadavpur University and University of Calcutta for providing research facilities. The authors have no other relevant affiliations or financial involvement with any organization or entity with a financial interest in or financial conflict with the subject matter or materials discussed in the manuscript apart from those disclosed.

No writing assistance was utilized in the production of this manuscript.

Ethical conduct of research

The authors state that they have obtained appropriate institutional review board approval or have followed the principles outlined in the Declaration of Helsinki for all human or animal experimental investigations. In addition, for investigations involving human subjects, informed consent has been obtained from the participants involved.

References

Papers of special note have been highlighted as: • of considerable interest

1. Park SY, Jun JA, Jeong KJ *et al.* Histone deacetylases 1, 6 and 8 are critical for invasion in breast cancer. *Oncol.Rep.* 25(6), 1677–1681 (2011).
2. Fabre B, Filipiak K, Zapico JM *et al.* Progress towards water-soluble triazole-based selective MMP-2 inhibitors. *Org. Biomol. Chem.* 11(38), 6623–6641 (2013).
3. Halder AK, Mallick S, Shikh D *et al.* Design of dual MMP-2/HDAC8 inhibitors by pharmacophore mapping, molecular docking, synthesis and biological activity. *RSC Adv.* 5(88), 72373–72386 (2015).
4. Overall CM, Kleifeld O. Tumour microenvironment – opinion: validating matrix metalloproteinases as drug targets and anti-targets for cancer therapy. *Nat. Rev. Cancer* 6(3), 227–239 (2006).
5. Adhikari N, Mukherjee A, Saha A *et al.* Arylsulfonamides and selectivity of matrix metalloproteinase-2: an overview. *Eur. J. Med. Chem.* 129, 72–109 (2017).
6. Ranogajec I, Jakić-Razumović J, Puzović V *et al.* Prognostic value of matrix metalloproteinase-2 (MMP-2), matrix metalloproteinase-9 (MMP-9) and aminopeptidase N/CD13 in breast cancer patients. *Med. Oncol.* 29(2), 561–569 (2012).
7. Amin SA, Adhikari N, Jha T. Is dual inhibition of metalloenzymes HDAC-8 and MMP-2 a potential pharmacological target to combat hematological malignancies? *Pharmacol. Res.* 122, 8–19 (2017).
8. Amin SA, Adhikari N, Jha T. Structure-activity relationships of HDAC8 inhibitors: non-hydroxamates as anticancer agents. *Pharmacol. Res.* 131, 128–142 (2018).
9. Mittal K, Ebos J, Rini B. Angiogenesis and the tumor microenvironment: vascular endothelial growth factor and beyond. *Semin. Oncol.* 41(2), 235–251 (2014).
10. Amin SA, Adhikari N, Jha T. Structure-activity relationships of hydroxamate-based histone deacetylase-8 inhibitors: reality behind anticancer drug discovery. *Future Med. Chem.* 9(18), 2211–2237 (2017).
11. Amin SA, Adhikari N, Jha T. Design of aminopeptidase N inhibitors as anti-cancer agents. *J. Med. Chem.* 61(15), 6468–6490 (2018).

• **An interesting review highlighting anticancer APN inhibitors.**

12. Amin SA, Adhikari N, Jha T. Diverse classes of HDAC8 inhibitors: In search of molecular fingerprints that regulate the activity. *Future Med. Chem.* 10(13), 1589–1602 (2018).
13. Jha T, Adhikari N, Saha A *et al.* Multiple molecular modelling studies on some derivatives and analogues of glutamic acid as matrix metalloproteinase-2 inhibitors. *SAR QSAR Environ. Res.* 29(1), 43–68 (2018).
14. Micelli C, Rastelli G. Histone deacetylases: structural determinants of inhibitor selectivity. *Drug Discov. Today* 20(6), 718–735 (2015).
15. Deschamps N, Simões-Pires CA, Carrupt PA *et al.* How the flexibility of human histone deacetylases influences ligand binding: an overview. *Drug Discov.Today* 20(6), 736–742 (2015).
16. Chakrabarti A, Melesina J, Kolbinger FR *et al.* Targeting histone deacetylase 8 as a therapeutic approach to cancer and neurodegenerative diseases. *Future Med. Chem.* 8(13), 1609–1634 (2016).
17. Chakrabarti A, Oehme I, Witt O *et al.* HDAC8: a multifaceted target for therapeutic interventions. *Trends Pharmacol. Sci.* 36(7), 481–492 (2015).

• **An important review focusing biological and therapeutic implication of HDAC8.**

18. Halder AK, Saha A, Jha T. Exploration of structural and physicochemical requirements and search of virtual hits for aminopeptidase N inhibitors. *Mol. Divers.* 17(1), 123–137 (2013).
19. Terauchi M, Kajiyama H, Shibata K *et al.* Inhibition of APN/CD13 leads to suppressed progressive potential in ovarian carcinoma cells. *BMC Cancer* 7(1), 140 (2007).
20. Liu CC, Chang TC, Lin YT *et al.* Paracrine regulation of matrix metalloproteinases contributes to cancer cell invasion by hepatocellular carcinoma-secreted 14–3-3σ. *Oncotarget* 7(24), 36988–36999 (2016).
21. Liang W, Gao B, Xu G *et al.* Possible contribution of aminopeptidase N (APN/CD13) to migration and invasion of human osteosarcoma cell lines. *Int. J. Oncol.* 45(6), 2475–2485 (2014).
22. Liu LT, Chang HC, Chiang LC *et al.* Histone deacetylase inhibitor up-regulates RECK to inhibit MMP-2 activation and cancer cell invasion. *Cancer Res.* 63(12), 3069–3072 (2003).
23. Meng N, Li Y, Zhang H *et al.* RECK, a novel matrix metalloproteinase regulator. *Histol. Histopathol.* 23(8), 1003–1010 (2008).
24. Takahashi C, Sheng Z, Horan TP *et al.* Regulation of matrix metalloproteinase-9 and inhibition of tumor invasion by the membrane-anchored glycoprotein RECK. *Proc. Natl Acad. Sci USA* 95(22), 13221–13226 (1998).
25. Oh J, Takahashi R, Kondo S *et al.* The membrane anchored MMP inhibitor RECK is a key regulator of extracellular matrix integrity and angiogenesis. *Cell* 107(6), 789–800 (2001).
26. Mook OR, Frederiks WM, Van Noorden CJ. The role of gelatinases in colorectal cancer progression and metastasis. *Biochim. Biophys. Acta* 1705(2), 69–89 (2004).
27. Masui T, Doi R, Koshiba T *et al.* RECK expression in pancreatic cancer: Its correlation with lower invasiveness and better prognosis. *Clin.Cancer Res.* 9(5), 1779–1784 (2003).
28. van der Jagt MF, Sweep FC, Waas ET *et al.* Correlation of reversion-inducing cysteine-rich protein with kazal motifs (RECK) and extracellular matrix metalloproteinase inducer (EMMPRIN), with MMP-2, MMP-9, and survival in colorectal cancer. *Cancer Lett.* 237(2), 289–297 (2006).
29. Cho YB, Lee WY, Song SY *et al.* Matrix metalloproteinase-9 activity is associated with poor prognosis in T3–T4 node-negative colorectal cancer. *Hum. Pathol.* 38(11), 1603–1610 (2007).
30. Chen Y, Tsai YH, Tseng SH. HDAC inhibitors and RECK modulate endoplasmic reticulum stress in tumor cells. *Int. J. Mol. Sci.* 18(2), E258 (2017).
31. Chen Y, Tseng SH. The potential of RECK inducers as antitumor agents for glioma. *Anticancer Res.* 32(7), 2991–2998 (2012).
32. Jeon HW, Lee YM. Inhibition of histone deacetylase attenuates hypoxia-induced migration and invasion of cancer cells via the restoration of RECK expression. *Mol. Cancer Ther.* 9(5), 1361–1370 (2010).
33. Mani SK, Kern CB, Kimbrough D *et al.* Inhibition of class I histone deacetylase activity represses matrix metalloproteinase-2 and -9 expression and preserves LV function postmyocardial infarction. *Am. J. Physiol. Circ. Physiol.* 308(11), H1391–H1401 (2015).
34. Wang F, Qi Y, Li X, He W, Fan QX, Zong H. HDAC inhibitor trichostatin A suppresses esophageal squamous cell carcinoma metastasis through HADC2 reduced MMP-2/9. *Clin. Invest. Med.* 36(2), E87–E94 (2013).
35. Balasubramanian S, Ramos J, Luo W *et al.* A novel histone deacetylase 8 (HDAC8)-specific inhibitor PCI-34051 induces apoptosis in T-cell lymphomas. *Leukemia* 22(5), 1026–1034 (2008).
36. Mukherjee A, Adhikari N, Jha T. A pentanoic acid derivative targeting matrix metalloproteinase-2 (MMP-2) induces apoptosis in a chronic myeloid leukemia cell line. *Eur. J. Med. Chem.* 141, 37–50 (2017).
37. Gottlieb E, Armour SM, Harris MH *et al.* Mitochondrial membrane potential regulates matrix configuration and cytochrome c release during apoptosis. *Cell Death Differ.* 10(6), 709–717 (2003).
38. Adhikari N, Halder AK, Mallick S *et al.* Robust design of some selective matrix metalloproteinase-2 inhibitors over matrix metalloproteinase-9 through i*n silico*/fragment-based lead identification and *de novo* lead modification: syntheses and biological assays. *Bioorg. Med. Chem.* 24(18), 4291–4309 (2016).
39. Adhikari N, Amin SA, Saha A *et al.* Understanding chemico-biological interactions of glutamate MMP-2 inhibitors through rigorous alignment-dependent 3D-QSAR analyses. *Chem. Select* 2(26), 7888–7898 (2017).
40. Maestro Software, Schrodinger Inc., NY, USA (2018).
41. Pantelić N, Zmejkovski BB, Kolundžija B *et al. In vitro* antitumor activity, metal uptake and reactivity with ascorbic acid and BSA of some gold(III) complexes with *N,N'*-ethylenediamine bidentate ester ligands. *J. Inorg. Biochem.* 172, 55–66 (2017).